Chapter 6 Earthquakes

[Public Notice] (Earthquake Ground Motions)

Article 16

1 Level 1 earthquake ground motion s shall be appropriately set in the form of probabilistic time histories based on the results of earthquake observations, taking into consideration the source, path and site effects.

2 Level 2 earthquake ground motions shall be appropriately set in the form of time histories based on the results of earthquake observations and the source parameters of scenario earthquakes, taking into consideration the source, path and site effects.

[Interpretation]

7. Setting of Natural Conditions

(6) Items related to Earthquakes (Article 6 of the Ministerial Ordinance and the interpretations related to Articles 16 and 17 of the Public Notice)

① **The depth for setting earthquake ground motions**

The time histories of Level 1 and Level 2 earthquake ground motions shall be specified at the engineering bedrock as defined in ②. If it is necessary to set earthquake ground motions at depths other than the engineering bedrock in the performance verification of facilities subjected to the technical standards, the earthquake ground motions at such depths shall be set through one-dimensional earthquake response analyses of the ground, etc. in which the design ground motion at the engineering bedrock is used as an input motion.

② **Engineering bedrock**

The engineering bedrock shall be the upper boundary of the layers that can be categorized as one of the following:

• bedrock;

• a sandy layer with standard penetration test values (*SPT-N* values) of 50 or more;

• a cohesive soil layer with an unconfined compression strength of 650 [kN/m^2] or more; and

• a layer with a shear wave (S wave) velocity of 300 [m/s] or more.

③ **Site effects**

The site effects shall be appropriately evaluated taking into account the results of earthquake observations at the site of construction and/or in its vicinity.

④ **Time histories of earthquake ground motions**

In the performance verification of facilities subjected to the technical standards, Level 1 and Level 2 earthquake ground motions shall be appropriately set at the engineering bedrock in the form of acceleration, velocity or displacement time histories as needed, taking into account the results of earthquake observations and geotechnical properties at the site of construction.

⑤ **Level 1 earthquake ground motions**

a) Level 1 earthquake ground motions

Level 1 earthquake ground motions shall be set on the assumption that the earthquakes occur in the areas around the port under consideration in accordance with a stationary Poisson process, which means that these earthquakes occur randomly over time, regardless of the historical records. Thus, according to the above definition of Level 1 earthquake ground motions, even an earthquake such as the Nankai Trough earthquake, which is expected to occur in the near future based on the historical records, may not be considered in setting Level 1 earthquake ground motions if its average recurrence interval is longer, to some extent, than the return period of Level 1 earthquake ground motions.

b) Probabilistic time histories

Probabilistic time histories are the time histories of earthquake ground motions set through a probabilistic seismic hazard analysis which considers the probability of earthquake occurrence. The probabilistic time histories of Level 1 earthquake ground motions shall be set on the basis of uniform hazard Fourier spectra, in which any frequency components have identical return periods in order to appropriately consider the frequency content of earthquake ground motions.

⑥ **Return period**

The return period of the uniform hazard Fourier spectra for setting Level 1 earthquake ground motions shall be set at 75 years.

⑦ **Level 2 earthquake ground motions**

a) Level 2 earthquake ground motions

In setting Level 2 earthquake ground motions, scenario earthquakes shall be selected from the following six types of earthquakes, taking into account the peak amplitude, frequency content and duration of resultant ground motions and their potential effects on structures. The selection of the scenario earthquakes shall be based on a comprehensive evaluation of the survey results by government agencies such as the Central Disaster Management Council and the Headquarters for Earthquake Research Promotion, and of regional disaster prevention plans.

i) Recurrence of past damaging earthquakes

ii) Earthquakes caused by active faults

iii) Other earthquakes expected from seismological and/or geological point of view

iv) Scenario earthquakes hypothesized by government agencies such as the Central Disaster Management Council and the Headquarters for Earthquake Research Promotion

v) Scenario earthquakes hypothesized by local governments

vi) M6.5 earthquake just beneath the site

b) Source parameters

When setting Level 2 earthquake ground motions, outer and inner source parameters shall be appropriately set in accordance with the type of the scenario earthquake.

1 Earthquake Ground Motions

1.1 General

In general, earthquake ground motions are affected by three factors, namely, the source, path and site effects (**Fig. 1.1.1**). The source effects can be defined as the characteristics of seismic waves generated at the earthquake source as a result of a rupture process on the fault. The path effects can be defined as the attenuation and deformation of seismic waves during their propagation from the source to the upper boundary of the seismological bedrock below the site. The site effects can be defined as the influence of sediments above the seismological bedrock on the seismic waves. The seismological bedrock can be defined as the layers having a shear wave velocity greater than or equal to 3 km/s and it is often composed of granite in Japan. Among those effects, the influence of sediments above the seismological bedrock is so significant that it is important to accurately evaluate the site effects to estimate ground motions during future earthquakes at a construction site. Regarding the site effects, it has been increasingly recognized that, in addition to the influence of shallower sediments above the engineering bedrock, the influence of deeper sediments below the engineering bedrock is also significant[1)]. In-situ earthquake observations and microtremor measurements can be a useful tool to evaluate the site effects. The existence of sediments affects not only the amplitude but also the temporal characteristics of earthquake ground motions. In the following, its effects on the amplitude will be called the “site amplification factors”. Its effects on earthquake ground motions in general will be simply referred to as the “site effects.”

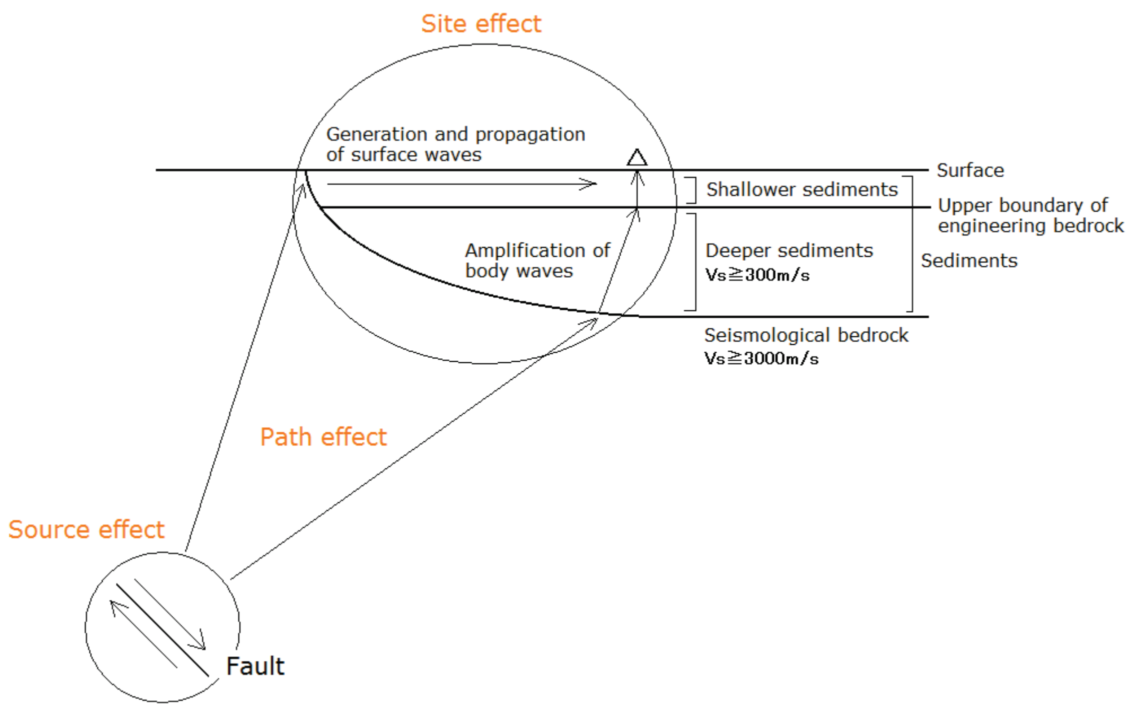

Fig. 1.1.1 Source, path and site effects

1.1.1 Source effects

(1) Omega-square model

The omega-square model[2)] has been widely used to represent the source effects of earthquake ground motions. According to the omega-square model, the acceleration Fourier spectrum of a seismic wave radiated at the earthquake source, *i.e.*, the acceleration source spectrum can be represented as;

$$S(f) = C\frac{M_0}{4\pi\rho V_S^3}\frac{(2\pi f)^2}{1+(f/f_c)^2}, \tag{1.1.1}$$

where

$S(f)$: Acceleration source spectrum

M_0 : Seismic moment

f : Frequency

f_c : Corner frequency

ρ : Density in the seismological bedrock

V_s : Shear wave velocity in the seismological bedrock

C : Constant (see **equation (1.3.5)**)

Fig. 1.1.2 shows the displacement, velocity and acceleration source spectra following the omega square model. **Equation (1.1.1)** and **Fig. 1.1.2** indicate that the acceleration source spectra following the omega square model are proportional to the squared frequency for frequencies below f_c and are constant for frequencies above f_c. Thus, f_c corresponds to the corner of the source spectrum.

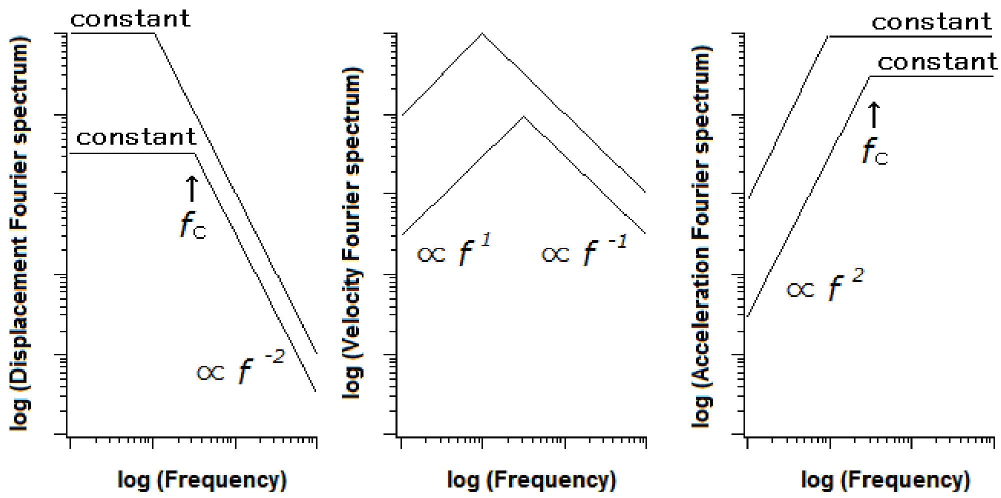

Fig. 1.1.2 Displacement, velocity and acceleration source spectra following the omega-square model

Seismic moment[3)] M_0 is an indicator of the size of an earthquake. It is defined as follows:

$$M_0 = \mu A D_0 , \tag{1.1.2}$$

where

μ : Shear modulus of rocks in the source region

A : Area of rupture along the fault

D_0 : Averaged final slip on the fault

On average, f_c is inversely proportional to $M_0^{1/3}$. Therefore, according to the omega-square model, the Fourier spectrum of a seismic wave radiated at the earthquake source is proportional to M_0 in the long period range, *i.e.*, in the low frequency range, while it is proportional to $M_0^{1/3}$ in the short period range, *i.e.*, in the high frequency range. Because M_0 is increased approximately by a factor of 30 for a unit increase in magnitude, the long and short period components of the seismic wave radiated at the earthquake source are increased approximately by a factor of 30 and 3, respectively, indicating that the long period components are more significantly increased than the short period components for a unit increase in magnitude. Therefore, when designing structures susceptible to long-period ground motions such as tall buildings, long bridges, oil tanks and base-isolated structures, it is important to pay attention especially to earthquakes with a great magnitude.

(2) Directivity

The source of a large earthquake is not just one point but a fault surface with finite dimension. Rupture starts at one point and propagates on the fault. Because the velocity of rupture propagation is more or less similar to the shear wave velocity in the source region, if the port is located in the direction of rupture propagation, seismic waves radiated at different parts on the fault arrive almost simultaneously, causing an intense ground motion. This effect is called the "forward directivity effect". It has been suggested that the destructive ground motions in the City of Kobe during the 1995 Hyogo-ken Nanbu (Kobe) earthquake (M7.3) were partly caused by this effect as the rupture started below Akashi Strait and propagated toward the City of Kobe[4)].

It has also been suggested that, in a region affected by the forward directivity effect, out of two horizontal components of ground motions, the component perpendicular to the strike of the fault tends to be stronger than the other component[5)6)7)8)]. When planning an important quay wall such as a high seismic resistant quay wall near an active fault, this tendency can be utilized to reduce potential damage to the quay wall by locating the facility in such a way that its face-line orientation be advantageous for coming strong motions; it is advantageous to orient its face line perpendicular to the strike of the fault[9)10)]. A high seismic resistant quay wall that was located at Maya Terminal in Kobe Port during the 1995 Hyogo-ken Nanbu earthquake could be mentioned as an example of a quay wall that avoided significant damage partly because of its orientation. Although many other quay walls in Kobe Port suffered large deformation of several meters, the quay wall at Maya Terminal suffered relatively slight deformation of approximately 1 m partly because its face line was oriented perpendicular to the causative Rokko-Awaji fault system and it could avoid the action of strongest ground motions, although the reinforcement of the structure also contributed to the relatively slight damage.

(3) Asperity

It has been revealed that slip on the fault of a large earthquake is not uniform but heterogeneous. For crustal earthquakes, regions on the fault with significantly large slip are called the "asperities". It is inevitable to consider the existence of asperities to explain intense ground motions such as those observed in the City of Kobe during the 1995 Hyogo-ken Nanbu earthquake[4)]. Two types of fault models have been used to represent slip heterogeneity on the fault, namely the "variable slip model" in which the slip is a continuous function on the fault and the "characterized source model" in which asperities are represented by rectangles. However, current knowledge tells us that, for a huge subduction earthquake, regions on the fault with large slip do not necessarily correspond to regions that generate strong ground motions[11)].

During subduction earthquakes such as the 2011 Tohoku earthquake, pulse-like ground motions with periods of one to several seconds have often been observed[12)13)14)]. The SPGA model[12)13)] is a source model which is capable of fully reproducing the characteristics of ground motions of a subduction earthquake in the period range with engineering importance including those pulses. The model involves regions called "SPGAs (Strong-motion Pulse Generation Areas)", each having a dimension of several kilometers.

1.1.2 Path effects

As for the path effects on the amplitude of earthquake ground motions, both geometrical spreading of body waves ($1/r$) and inelastic damping are commonly considered as follows:

$$P(f) = \frac{1}{r}\exp\left(-\pi f r / Q V_S\right), \qquad \textbf{(1.1.3)}$$

where

$P(f)$: Path effect

r : Source-to-site distance

Q : Quality factor

Quality factor is a quantity to represent the extent of inelastic damping in the propagation path due to scattering and the conversion of elastic energy into heat: greater quality factor implies smaller inelastic damping. It should be noted that, at greater distances from the source, the geometrical spreading term in the form of $1/r$ does not apply due to the existence of reverberating waves in the crust such as L_g waves[15)].

1.1.3 Site effects

(1) Fundamental characteristics of site effects

The existence of sediments above the seismological bedrock (**Fig. 1.1.1**) has significant effects on the amplitude, frequency content and duration of earthquake ground motions. These effects are referred to as the "site effects." The relationship between the subsurface structure and the site effects is summarized in **Fig. 1.1.3**.

① At the outcrop of the seismological bedrock or a layer equivalent to it, ground motions are relatively weak.

② If the sediments above the seismological bedrock are thin, predominantly short period ground motions are observed, because the natural period of the sediments is short.

③ If the sediments above the seismological bedrock are thick, predominantly long period ground motions are observed, because the natural period of the sediments is long.

④ If the sediments have a closed shape, long duration ground motions are observed, because the seismic waves are easily trapped and continue reverberation within the sediments.

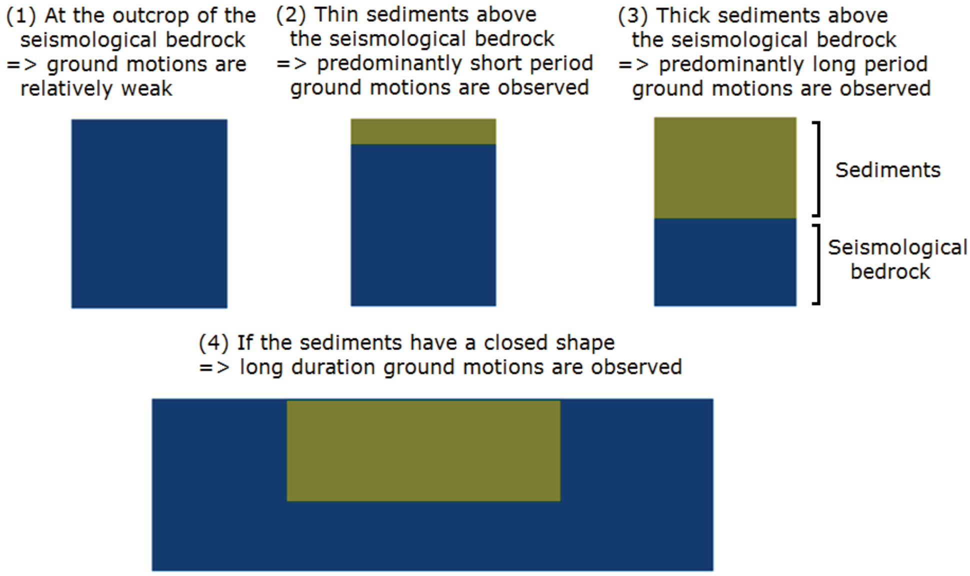

Fig. 1.1.3 Relationship between the subsurface structure and the characteristics of ground motions

There have been a lot of case histories in which earthquake ground motions were significantly affected by the existence of sediments. For example, it has been suggested that the "damage belt" in the City of Kobe during the 1995 Hyogo-ken Nanbu earthquake was generated partly because pulse-like ground motions with periods of 1-2 s were amplified by the sediments below the City of Kobe[4]. Comparison of observed ground motions at strong motion stations around the Port of Sakai (**Fig. 1.1.4**) during the 2000 Tottori-ken Seibu earthquake (M7.3) revealed that peak ground velocities were four times greater for the two stations in the plains of Yumigahama Peninsula (Sakaiminato-G and JMA) than for the two stations in mountainous Shimane Peninsula (SMN001 and SMNH10) (**Fig. 1.1.5**). The difference can be attributed to the amplification of seismic waves due to the existence of sediments below Yumigahama Peninsula. The damage was also concentrated in the City of Sakaiminato in Yumigahama Peninsula. The existence of sediments has such significant effects on strong ground motions that it is fundamentally important to appropriately consider the site effects to evaluate strong ground motions during future large earthquakes. In this regard, in addition to the influence of shallower sediments above the engineering bedrock, it is also important to consider the influence of deeper sediments below the engineering bedrock[1].

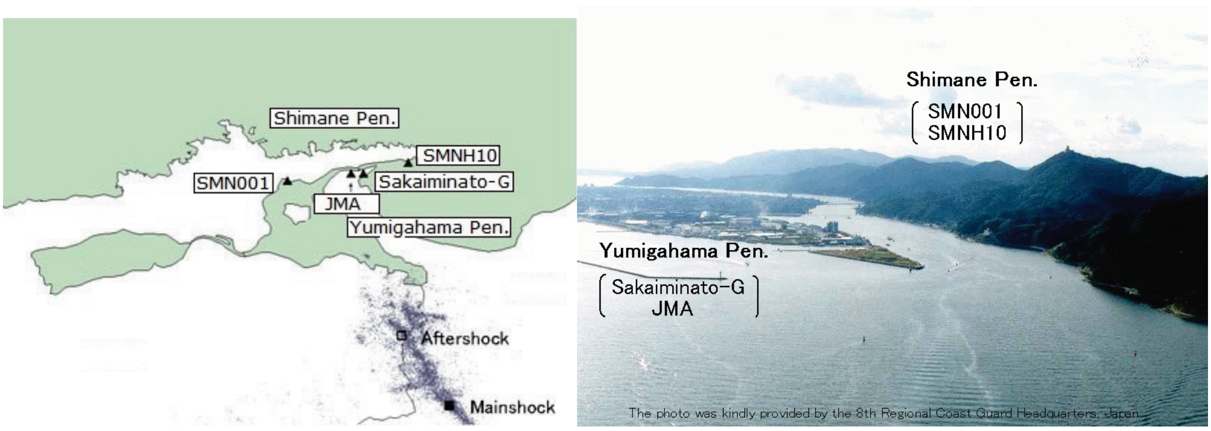

Fig. 1.1.4 Topography around the Port of Sakai and strong motion stations

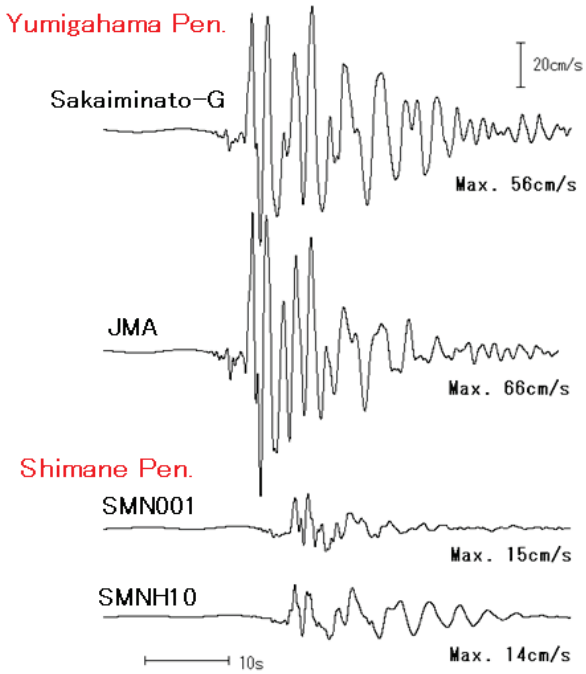

Fig. 1.1.5 Velocity waveforms for the fault-normal components observed around the Port of Sakai during the 2000 Tottori-ken Seibu earthquake

The frequency content of strong ground motions is also significantly affected by the existence of sediments. **Fig. 1.1.6** compares the Fourier spectra of past major strong motion records obtained at Hachinohe Port and Kansai International Airport. At Hachinohe Port, both of the Fourier spectra for the 1968 Tokachi-oki earthquake (M7.9) and the 1994 Sanriku-haruka-oki earthquake (M7.5) were characterized by a peak at the frequency of 0.4 Hz, *i.e.*, the period of 2.5 seconds. It has been revealed that this predominant period at Hachinohe Port is due to the subsurface geological structure below Hachinohe Port[16)]. On the other hand, at Kansai International Airport, both of the Fourier spectra for the 1995 Hyogo-ken Nanbu earthquake and the 2000 Tottori-ken Seibu earthquake were characterized by a peak at the frequency of 0.2 Hz, *i.e.*, the period of 5 seconds. The site-specific nature of the predominant period of ground motions can be attributed to the site effects. Knowing the predominant period of ground motions at a construction site can contribute to the safety of a structure by, for example, enabling the engineers to avoid resonance effects due to the coincidence of the natural period of the structure and the predominant period of ground motions.

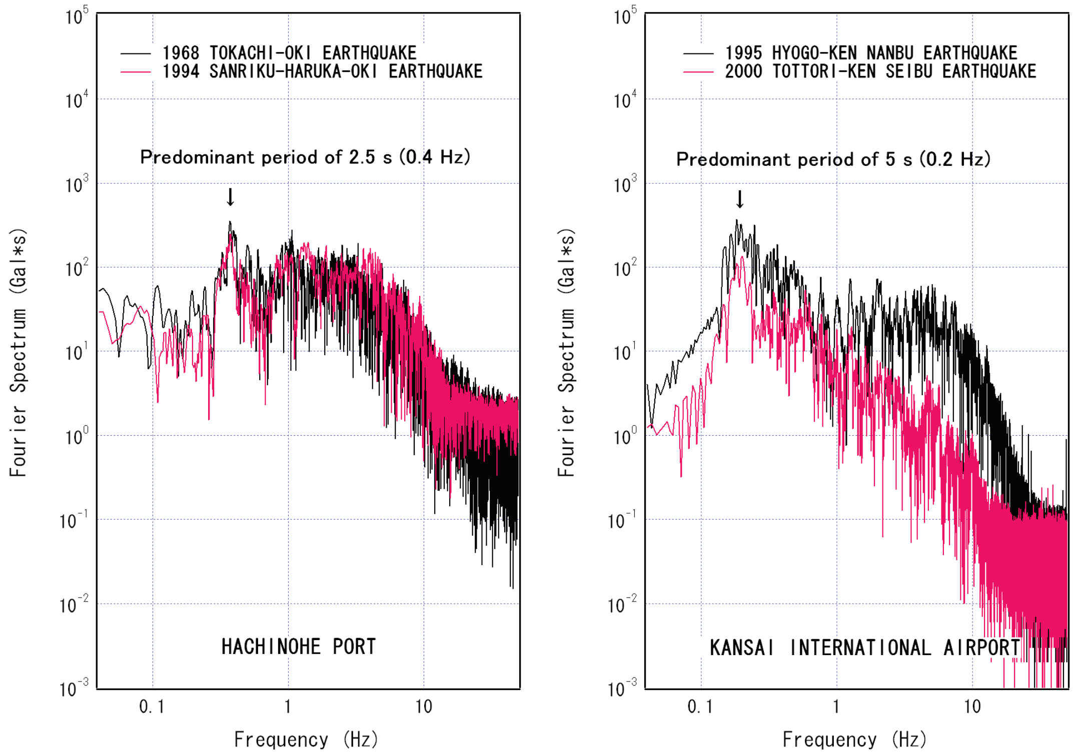

Fig. 1.1.6 Fourier spectra of past major strong motion records obtained at Hachinohe Port (NS component) and Kansai International Airport (Runway-normal component)

(2) Site effects all over Japan

The site effects can be most reliably evaluated by conducting earthquake observations. In Japanese ports and harbours, strong-motion observations have been conducted (**Fig. 1.1.7**). Strong-motion observations can be distinguished from other types of earthquake observations by the fact that they are conducted with instruments that are operable under severe earthquakes. Although the primary purpose of the Strong-Motion Earthquake Observation in Japanese Ports is to observe damaging ground motions due to severe earthquakes, weak-motion records daily obtained by the network can be used to evaluate site effects. The records obtained by the network can be downloaded from the website of the Ports and Harbours Bureau, Ministry of Land, Infrastructure, Transport and Tourism at http://www.mlit.go.jp/kowan/kyosin/eq.htm.

Nozu et al.[17)] applied a kind of regression analysis known as the “generalized inversion” to a dataset composed of strong motion data from the Strong-Motion Earthquake Observation in Japanese Ports as well as K-NET[18)] and KiK-net[19)] and evaluated the site amplification factors at strong motion stations all over Japan at the ground surface with respect to the seismological bedrock. The results are available on a CD attached to their report[17)] or at the PARI website at https://www.pari.go.jp/bsh/jbn-kzo/jbn-bsi/taisin/siteamplification_jpn.html. **Fig. 1.1.8** shows the strong motion stations for which the generalized inversion was applied[17)].

Fig. 1.1.7 Strong-Motion Earthquake Observation in Japanese Ports

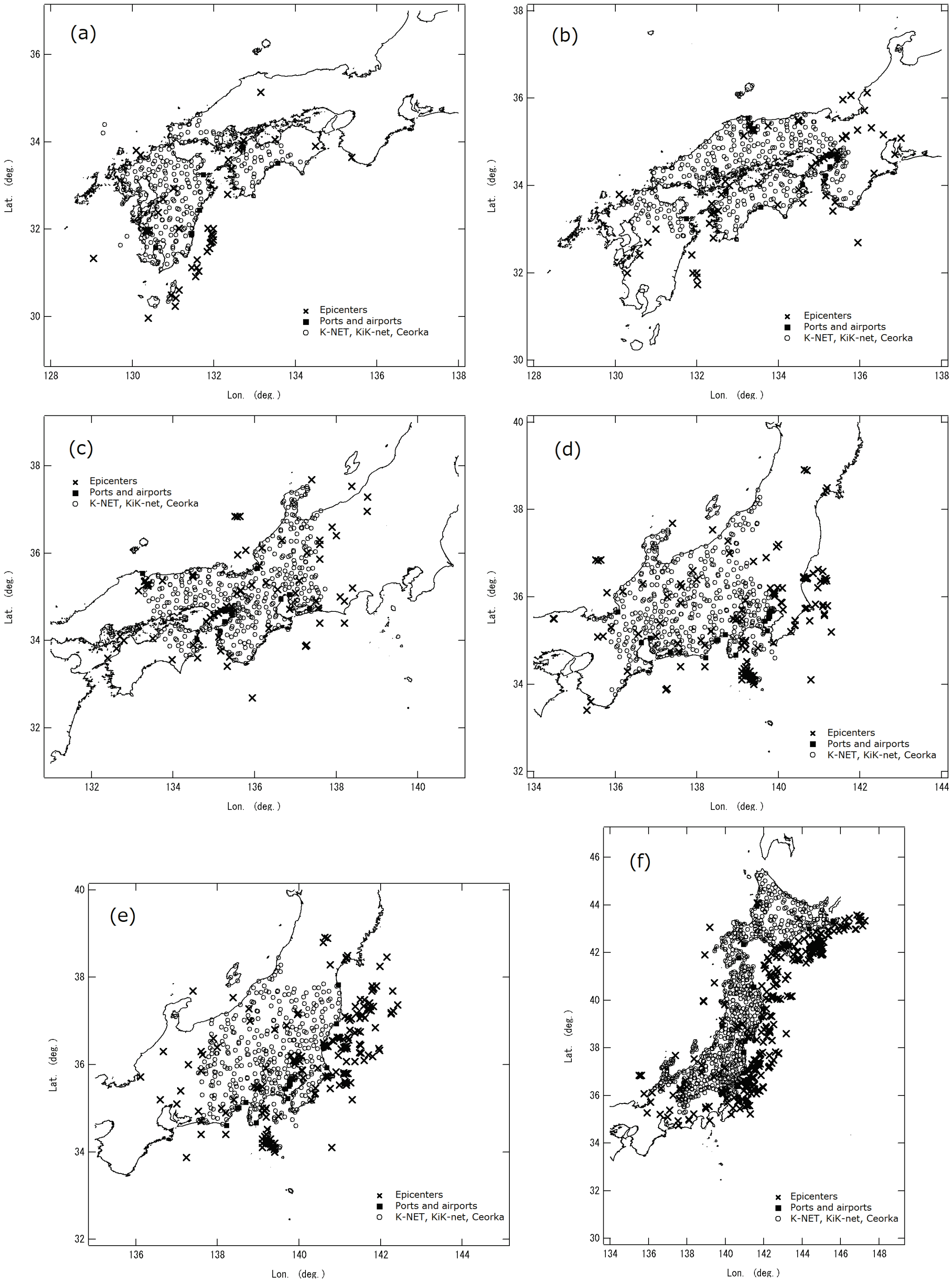

Fig. 1.1.8 Strong motion stations for which the generalized inversion was applied[17].

The inversion was separately applied to regions shown in (a) – (f).
Each panel shows the epicenters of the earthquakes and the strong motion stations.

Typical results from their report[17] are shown in **Fig. 1.1.9** and **Fig. 1.1.10**.

In the northern part of Chugoku District, Japan, alluvial plains are distributed around Lake Nakaumi and Lake Shinji, including cities like Yonago, Sakaiminato, Matsue and Izumo. The left panel of **Fig. 1.1.9** shows the strong motion stations located in the alluvial plains and in the mountains to the south of the plains. The right panel of **Fig. 1.1.9** shows the site amplification factors at those stations. At the stations located in the alluvial plains, namely, TTR008, SMN002, SMN005 and Sakaiminato-G, the site amplification factors include a peak exceeding 10 in the frequency range between 0.5 – 2 Hz, although the peak frequency depends on the site. On the other hand, at the stations located in the mountains, namely, TTR007, TTR009, SMN003, SMN004 and SMN016, the site amplification factors are around 1 – 2 in the frequency range below 1 Hz as shown by black lines in the right panel of **Fig. 1.1.9**, indicating that those stations are almost rock sites. Thus, the site amplification factors are significantly different between the plains and the mountains. At the stations located in the alluvial plains, the peak frequency depends on the site because of the difference of the thickness of the sediments below each site.

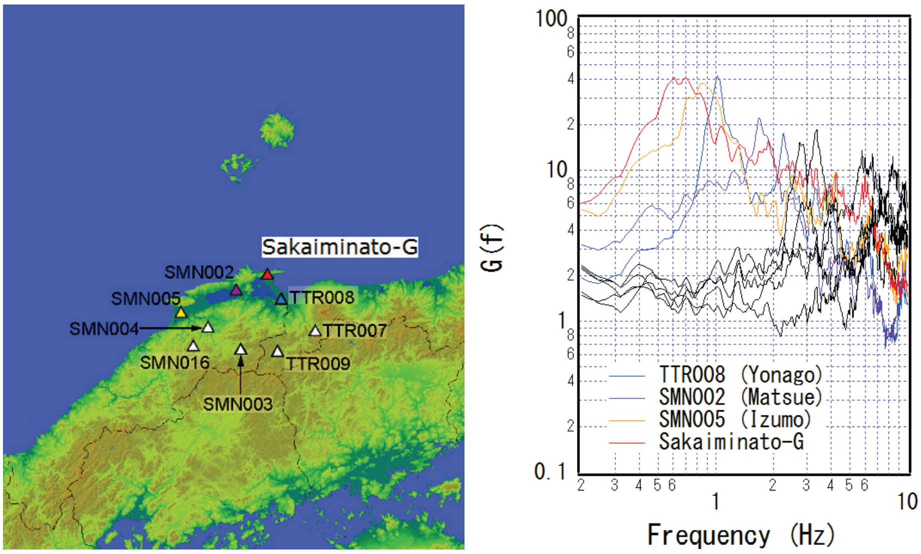

Fig. 1.1.9 Strong motion stations in the northern part of Chugoku District, Japan, and the site amplification factors at those stations

The left panel of **Fig. 1.1.10** shows the K-NET stations in Saitama Prefecture, Japan. The right panel of **Fig. 1.1.10** shows the site amplification factors at those stations. The site amplification factors are small at stations located in the mountains in the west such as SIT004, SIT005, SIT012 and SIT014 as shown by black lines, whereas the site amplification factors are large at stations located in the plains in the east such as SIT003, SIT008, SIT010 and SIT011 as shown by red lines. At SIT006 (Chichibu) located in a small basin surrounded by mountains, the site amplification factor is slightly larger than at the surrounding stations. Takemura[20] suggested that significant damage corresponding to seismic intensity of 6 in the Japanese scale occurred in the east of Saitama Prefecture during the 1923 Great Kanto earthquake. The region that suffered significant damage almost coincides with the region with large site amplification factors in **Fig. 1.1.10**.

Regarding the site amplification factors at strong motions stations, in addition to the above report[17], there are other published reports for the site amplification factors in Nansei Islands[21] and Northern Hokkaido[22], Japan.

Although strong motion stations look so densely located once plotted on a nationwide map as in **Fig. 1.1.8**, they are actually 20 – 30 km apart from each other. Therefore, the site amplification factor at a construction site cannot usually be revealed only by the existing strong motion networks. It is necessary to conduct in-situ earthquake observations and/or microtremor measurements to evaluate the site amplification factor. The details will be explained in **Part II, Chapter 6, 1.2.2 Evaluation of site amplification factors**.

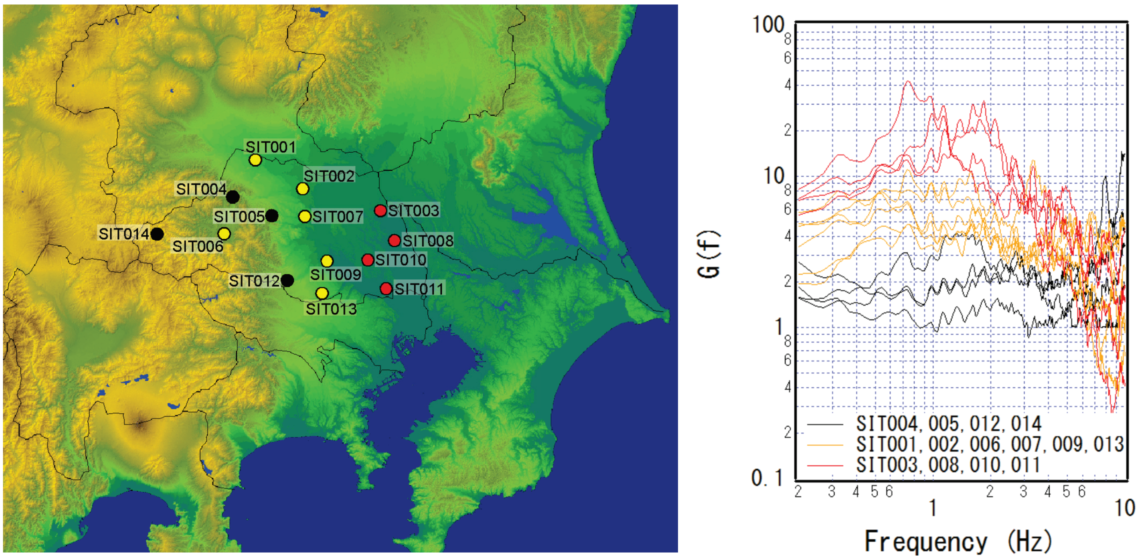

Fig. 1.1.10 K-NET stations in Saitama Prefecture, Japan, and the site amplification factors at those stations. (The red, yellow and black markers indicate strong motion stations with large, medium and small site amplification factors, respectively.)

1.1.4 Soil nonlinearity

In general, material properties of shallower sediments are dependent on their strain levels; under strong ground motions, the shear modulus decreases and the damping factor increases. These characteristics are called "soil nonlinearity". Nonlinear behavior of the soil can be easily detected by taking the surface to borehole Fourier spectral ratios of strong and weak motion records. **Fig. 1.1.11** shows the surface to borehole Fourier spectral ratios for all the records in 2003 with M5.0 or greater at Kushiro Port. The Fourier spectra for the EW and NS components were smoothed with moving average and their compositions were plotted. The thick line is for the September 26, 2003, Tokachi-oki earthquake (M8.0). Except for the M8.0 earthquake, the spectral ratios always had peaks at 1 Hz and 3 Hz, whereas the peaks shifted to lower frequencies for the M8.0 event. This is a typical example of soil nonlinearity.

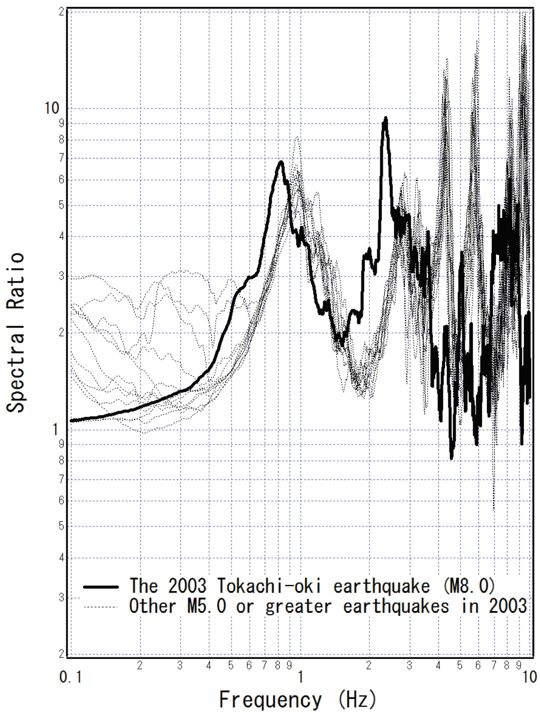

Fig. 1.1.11 Surface to borehole Fourier spectral ratios at Kushiro Port. All the records in 2003 with M5.0 or greater are plotted.

1.1.5 Spatial variation of earthquake ground motions

Spatial variation of earthquake ground motions can be an important issue to be considered in designing a long or a large structure such as a submerged tunnel or a buried pipeline. Horizontal heterogeneity of the ground within the dimension of a long or a large structure can cause spatial variation of earthquake ground motions. For a ground with less horizontal heterogeneity, horizontal wave propagation can be a major cause of spatial variation of earthquake ground motions. For details see **Part II, Chapter 6, 1.4 Spatial variation of earthquake ground motions for the performance verification of structures**.

1.2 Level-1 ground motions for the performance verification of structures

1.2.1 General

In general, level-1 ground motions are determined by means of a probabilistic seismic hazard analysis considering the source and path effects and the site amplification factor at the engineering bedrock with respect to the seismological bedrock. The ground motions to be determined are the so called "2E wave" [23)], which is the incident wave impinging at the surface of the engineering bedrock multiplied by 2.

Time history data of level-1 ground motions at major ports, etc. that were determined taking account of regional source and path effects are available at the website of the National Institute for Land and Infrastructure Management at http://www.ysk.nilim.go.jp/kakubu/kouwan/sisetu/sisetu.html. Detailed procedures for the determination can be found in Takenobu et al.[24)]. In some cases, however, it cannot be guaranteed that the site amplification factor that was used to calculate a level-1 ground motion be equivalent to the site amplification factor at a construction site. In that case, it is necessary to confirm this equivalence by using microtremor measurements. The details will be explained in **Reference (Part II), Chapter 1, 4.2 Microtremor measurements at the construction site** and in its vicinity. If they are equivalent, the existing level-1 ground motion available at the website can be used without correction. If they are not equivalent, it is necessary to evaluate the site amplification factor at the construction site by means of earthquake observations (See **Part II, Chapter 6, 1.2.2 Evaluation of site amplification factors (1)**) and/or microtremor measurements (See **Part II, Chapter 6, 1.2.2 Evaluation of site amplification factors (2)**) and to correct the existing level-1 ground motion before it is used for the design (See **Part II, Chapter 6, 1.2.4 Correction of level-1 ground motions**).

If it is difficult to conduct in-situ earthquake observations and/or microtremor measurements because of, for example, insufficient period of construction, the site amplification factor at the construction site can be evaluated by using an empirical relation (See **Part II, Chapter 6, 1.2.2 Evaluation of site amplification factors (3)**) based on the site amplification factor at a nearby strong motion station. In that case, it is important to recognize that the accuracy of the level-1 ground motion will be significantly degraded compared to cases with site amplification factors based on earthquake observations and/or microtremor measurements.

For the detailed procedures of the performance verification of a structure, see the descriptions in **Part III** depending on the type of the structure.

1.2.2 Evaluation of site amplification factors

(1) Evaluation of site amplification factors based on earthquake observations

It is desirable to evaluate the site amplification factor at a construction site based on earthquake observations. First, it is efficient to consider the availability of the existing strong motion stations of the Strong-Motion Earthquake Observation in Japanese Ports (see **Part II, Chapter 6, 1.1.3 Site effects**), K-NET[18)], KiK-net[19)] and the network of seismic intensity meters by the JMA and local governments. For that purpose, it is necessary to conduct microtremor measurements at the construction site and a nearby strong motion station (**Fig. 1.2.1**). If the characteristics of microtremors are similar between the two locations, it is reasonable to assume that the dynamic characteristics of the ground are similar between the two locations. In that case the site amplification factor at the nearby strong motion station can be used for the construction site. Details can be found in **Reference (Part II), Chapter 1, 4.2 Microtremor measurements at the construction site** and in its vicinity.

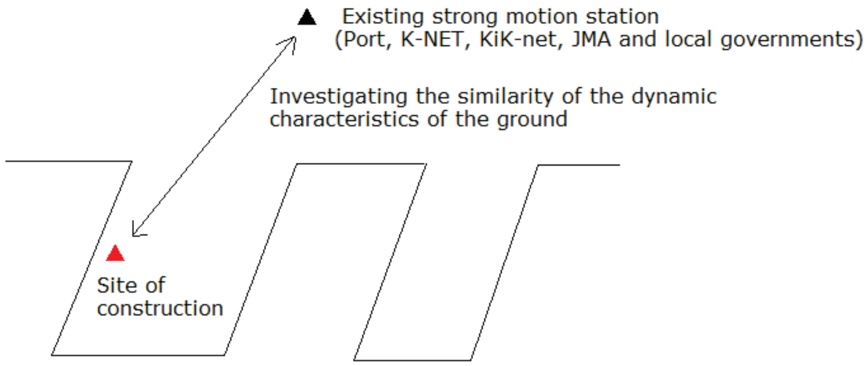

Fig. 1.2.1 Microtremor measurements at a construction site and a nearby strong motion station

However, if the results of the microtremor measurements indicate that the dynamic characteristics of the ground are different between the construction site and the nearby strong motion station, it is desirable to evaluate the site amplification factor at the construction site by means of in-situ earthquake observations, depending on the importance of the project. In that case, it is necessary to confirm that the dynamic characteristics of the ground are similar between the construction site and the site of the in-situ earthquake observations. Details of the evaluation of the site amplification factor by means of in-situ earthquake observations can be found in **Reference (Part II), Chapter 1, 4.3 Evaluation of site amplification factors based on in-situ earthquake observations**.

Once the site amplification factor at the ground surface with respect to the seismological bedrock is obtained based on earthquake observations, it can be divided by the transfer function between the engineering bedrock and the ground surface to obtain the site amplification factor at the engineering bedrock with respect to the seismological bedrock. For that purpose, the transfer function between the engineering bedrock and the ground surface can be evaluated based on geotechnical data at the observation site and the linear multiple reflection theory[23)25)] (see **Part II, Chapter 6, 1.2.3 Earthquake response analysis of the ground**). For this analysis, the damping factor of approximately 3% can be used. This value was selected because it is slightly larger than the values obtained in laboratory tests (*e.g*., Zen et al. [26)]) and it will result in conservative evaluation of the site amplification factor at the engineering bedrock with respect to the seismological bedrock.

(2) Evaluation of site amplification factors based on microtremor measurements

Microtremors can be defined as small vibrations of the ground under non-earthquake circumstances, which cannot usually be felt by human beings.

The horizontal to vertical spectral ratio of measured microtremors[27)], which is often called the “H/V spectrum”, is known to resemble the site amplification factor at the same site obtained from earthquake observations[28)]. As an example, the microtremor H/V spectra obtained at the Port of Kochi and nearby strong motion stations are compared with the site amplification factors obtained from earthquake observations[17)] in **Fig. 1.2.2**. The microtremor H/V spectra were calculated following the procedure described in **Reference (Part II), Chapter 1, 4.4 Evaluation of site amplification factors based on microtremor measurements**. At Kochi-G, the H/V spectrum has a clear peak at around 1.3 Hz, while the site amplification factor also has a peak almost at the same frequency. At KOC007, the H/V spectrum has a clear peak at around 1.6 Hz, while the site amplification factor also has a peak almost at the same frequency. At KOC005, the H/V spectrum does not have any clear peak, while the site amplification factor does not have any clear peak either. Thus, the microtremor H/V spectra capture the main features of the site amplification factors. A similar comparison is made for the Port of Wakayama and a nearby strong motion station in **Fig. 1.2.3**. Again, the microtremor H/V spectra capture the main features of the site amplification factors.

Thus, microtremor measurements can be a useful tool to reveal the major features of the site amplification factor at a construction site. Microtremor measurements can be used to answer such questions as “Is the amplification due to the existence of sediments anticipated at the construction site?” or “At which frequency does the amplification occur?”

On the other hand, following limitations are inherent in the evaluation of site amplification factors based on microtremor measurements. The first limitation concerns the height of the peak. As shown in **Fig. 1.2.2** and **Fig. 1.2.3**, peak frequencies are usually consistent between the microtremor H/V spectrum and the site amplification factor at the same site. However, there have been long discussions on the consistency of the peak heights. In fact, in some cases, the peak heights are reversed between the microtremor H/V spectrum and the site amplification factor as shown in **Fig. 1.2.2** for Kochi-G and KOC007. The second limitation is that higher mode peaks appearing in the site amplification factors are often not present in the microtremor H/V spectra. In the above examples, the peak around 3.3 Hz for the site amplification factor at Kochi-G and the peak around 1.2 Hz for the site amplification factor at Wakayama-G are not visible in the microtremor H/V spectra.

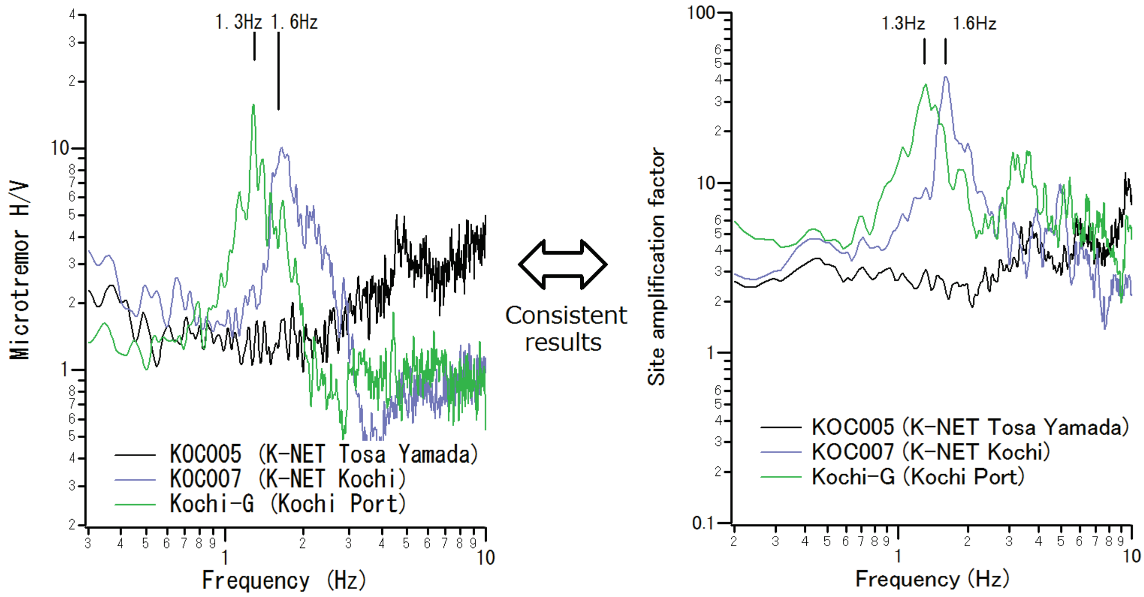

Fig. 1.2.2 Microtremor H/V spectra obtained at the Port of Kochi and nearby strong motion stations (left), compared with the site amplification factors obtained from earthquake observations[17] (right).

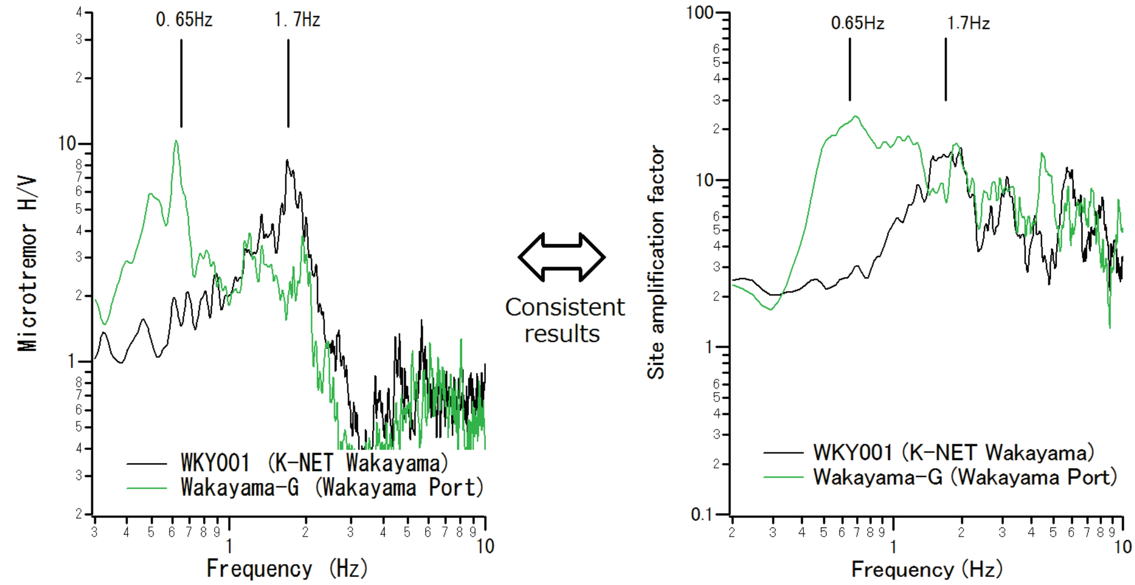

Fig. 1.2.3 Microtremor H/V spectra obtained at the Port of Wakayama and a nearby strong motion station (left), compared with the site amplification factors obtained from earthquake observations[17] (right).

Thus, uncertainties are inherent in the evaluation of site amplification factors based on microtremor measurements. Therefore, in the event of setting up design ground motions for a very important structure, it is desirable to evaluate the site amplification factor at the construction site based on earthquake observations. On the other hand, microtremor measurements are advantageous in setting up design ground motions for a number of facilities at the same time. Details of the evaluation of site amplification factors based on microtremor measurements can be found in **Reference (Part II), Chapter 1, 4.4 Evaluation of site amplification factors based on microtremor measurements**.

Once the site amplification factor at the ground surface with respect to the seismological bedrock is obtained based on microtremor measurements, the site amplification factor at the engineering bedrock with respect to the seismological bedrock can be obtained in a similar way as in the case of the site amplification factor at the ground surface evaluated based on earthquake observations (See **Part II, Chapter 6, 1.2.2 Evaluation of site amplification factors (1)**).

(3) Evaluation of site amplification factors without in-situ earthquake observations or microtremor measurements

An empirical relation[17)] between the site amplification factors at a port and a nearby K-NET or KiK-net strong motion station can be used to evaluate the site amplification factor at a construction site, if the site amplification factor is to be evaluated without in-situ earthquake observations or microtremor measurements. In that case, however, it is important to recognize that the accuracy of the ground motions will be significantly degraded compared to cases with site amplification factors based on earthquake observations and/or microtremor measurements. Possible effects of this degradation on the evaluation of quay-wall deformation are described in Nagao et al.[29)]. The empirical relation can be written as:

$$y = A + Bx$$
$$y = \log\big(GP(f)/GK(f)\big) \qquad \textbf{(1.2.1)}$$
$$x = \log GK(f),$$

where

GP : Site amplification factor at the engineering bedrock w.r.t. the seismological bedrock at a port

GK : Site amplification factor at the engineering bedrock w.r.t. the seismological bedrock at a nearby K-NET or KiK-net station

The frequency-dependent coefficients A and B are shown in **Fig. 1.2.4**. These coefficients were determined taking into account the general tendency of the site amplification factors at a port and nearby K-NET or KiK-net strong motion stations averaged over Japan.

In general, site amplification factors at the engineering bedrock at a port, estimated from site amplification factors at nearby K-NET or KiK-net stations using the coefficients in **Fig. 1.2.4**, exhibit large values at frequencies lower than 1 Hz. This is a consequence of a tendency that the seismological bedrock is generally deeper for ports than for K-NET or KiK-net stations. Thus, the coefficients in **Fig. 1.2.4** are not suitable for estimating site amplification factors outside a port.

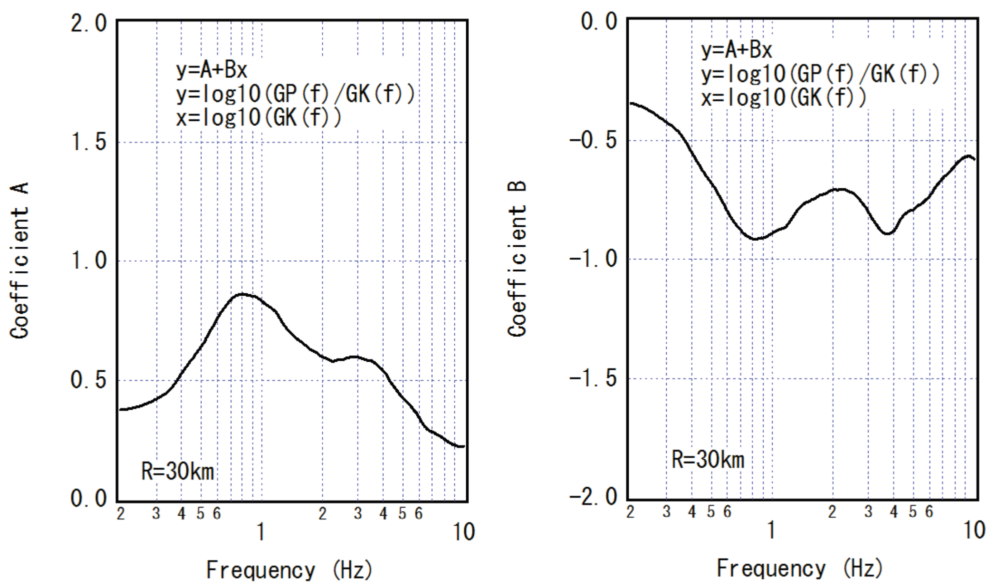

Fig. 1.2.4 Frequency-dependent coefficients A and B which specify the empirical relation between the site amplification factors at a port and a nearby K-NET or KiK-net strong motion station

1.2.3 Earthquake response analysis of the ground

In general, level-1 ground motions are specified in the form of so-called "2E wave" at the engineering bedrock, which is the incident wave impinging at the surface of the engineering bedrock multiplied by 2. Earthquake response analyses of the ground can be used to evaluate acceleration, velocity, displacement, shear stress and shear strain in the shallower sediments. Here, earthquake response analyses for this purpose will be described. Earthquake response analyses for the performance verification of facilities will be described in **Reference [Part III], Chapter 1, 2 Basic points of seismic response analyses**. While earthquake response analyses of the ground are usually conducted by appropriately modelling the shallower sediments above the engineering bedrock, there is a wide variation in the engineering bedrock itself in terms of its shear wave velocity; it is necessary to confirm that there is no significant difference in shear wave velocity between the layer regarded as the engineering bedrock in setting up the level-1 ground motion and the layer regarded as the engineering bedrock in the earthquake response analyses.

In the past, when earthquake response analyses were conducted for the prediction of liquefaction, the ground motions were converted to SMAC-B2 equivalent ground motions before they were used. This conversion is not necessary any more. In the past, existing strong motion records were adjusted to a specified PGA value and used for the earthquake response analyses. In that era, the specified PGA value was based on SMAC-B2 type accelerographs. This was the reason why the conversion into SMAC-B2 equivalent ground motions was necessary.

(1) Various earthquake response analyses of the ground

① **Domain of analysis**

There are one, two and three dimensional earthquake response analyses of the ground. In general, one dimensional analyses are used to calculate the response of horizontally layered natural or artificial deposits without a structure. For a horizontally layered ground often encountered in a coastal region, one dimensional analyses will give sufficiently accurate results.

In association with this, vertically travelling S waves are often considered in the earthquake response analyses of the ground. Because the shear wave velocities of the ground are generally small in the coastal regions, seismic rays become nearly vertical in the shallower sediments (**Fig. 1.1.1**). A similar tendency can also be found for surface waves: surface waves can also be considered as a superposition of elementary P and S waves in the shallower sediments and the rays of the elementary P and S waves also become nearly vertical near the surface. Thus, sufficiently accurate results can be obtained by simply considering vertically travelling S waves.

② **Stress-strain relations**

Earthquake response analyses of the ground can be categorized into equivalent linear analyses and purely nonlinear analyses from the viewpoint of how stress-strain relations are modelled. In the equivalent linear analyses, the dependence of the shear modulus and damping factor on the ground motion amplitude is considered (**Fig. 2.4.2** in **Part II, Chapter 3, 2.4.1 Parameters for dynamic deformation**), while they are assumed to be constant during the action of a ground motion. Obviously this assumption does not represent the actual situations. However, this assumption was introduced for convenience because of the limited performance of the computers in the days when the equivalent linear analyses were developed. On the other hand, in the purely nonlinear analyses, time dependence of the shear modulus, etc., during the action of a ground motion is considered. While it is necessary to use purely nonlinear analyses to represent the actual situations as accurately as possible, it has been postulated that the equivalent linear analyses give reasonable results as long as the strain level is within a certain range. The equivalent linear analyses are applicable if the stain level is less than 0.5 – 1%, depending on the method[30)31)]. If an equivalent linear analysis is used and a strain exceeding this level is obtained, then the analysis should be replaced by a purely nonlinear analysis.

In the equivalent linear analyses, following iterations are performed. First, at each step, the maximum shear strain at each layer (or at each element for two or three dimensional cases) is converted to the effective shear strain with the following equation:

$$\gamma_{eff} = \alpha \gamma_{\max} , \quad \textbf{(1.2.2)}$$

where

$\gamma_{\max}$: maximum shear strain

γ_{eff} : effective shear strain

α : a coefficient (typically 0.65)

Then, based on the effective shear strain, the shear modulus and damping factor are updated following the strain dependence shown in **Fig. 2.4.2** in **Part II, Chapter 3, 2.4.1 Parameters for dynamic deformation** before going to the next step. The iteration is repeated until the shear modulus converges. SHAKE[32] was the first computer program for the equivalent linear analysis of the ground. SHAKE has been widely used in practice partly because there was no competitive program for a while after SHAKE was initially developed. FLUSH[33], which can be regarded as a two dimensional version of SHAKE, has also been widely used. However, in recent years, problems inherent in SHAKE have gradually been revealed by comparing the results of SHAKE with actual ground motion records, etc.[34] One of the revealed shortcomings of SHAKE is its tendency to underestimate high frequency components. This in turn means that high frequencies tend to be overestimated when input ground motions at the engineering bedrock are to be estimated from surface records with SHAKE. In this regard, alternative programs such as FDEL[35] and DYNEQ[36] have been proposed, both of which can be regarded as improved versions of SHAKE. These programs mitigated the problem associated with high frequencies by introducing a frequency dependent effective strain instead of the effective strain defined in **equation (1.2.2)**.

Purely nonlinear analyses are applicable even when the stain level exceeds 0.5 – 1%. However, the accuracy of the results obviously depends on the appropriateness of the constitutive equations and model parameters. Various computer programs with various constitutive relations have been proposed for purely nonlinear analyses. It is important to use a computer program which successfully reproduced vertical array records with ground conditions and strain levels similar to the target problem[30].

Purely nonlinear analyses can be further categorized into total stress analyses and effective stress analyses. When the ground is subject to the generation of excess pore water pressure, the effective stress is decreased, resulting in the change of the shear modulus and damping factor of the ground and, ultimately, in the change of the response characteristics of the ground. Effective stress analyses can handle these situations and directly calculate the excess pore water pressure. On the other hand, total stress analyses, which do not calculate the excess pore water pressure, cannot consider the change of the response characteristics of the ground due to the change in the effective stress. In a calculation case with the excess pore water pressure ratio exceeding 0.5, it is anticipated that the results of total stress analyses become unrealistic. Thus, it is necessary to perform effective stress analyses to accurately trace the actual phenomena.

FLIP[37] is one of the computer programs for effective stress analyses. **Fig. 1.2.5** shows the application of FLIP ver.3.3 to the vertical allay records at Port Island in Kobe Port during the 1995 Hyogo-ken Nanbu earthquake[38]. At Port Island, ground motions were observed at four different depths, at GL-83 m, GL-32 m, GL-16 m and the ground surface. In this analysis, the observed ground motion at GL-83 m was used as an input ground motion and ground motions at other depths, namely, GL-32 m, GL-16 m and the ground surface were calculated. The results accurately reproduced the recorded ground motions. Such results, together with other results pertaining to, for example, the 1993 Kushiro-oki earthquake[39], indicate that FLIP is one of the programs that can generate reliable results as long as the model parameters are appropriately given.

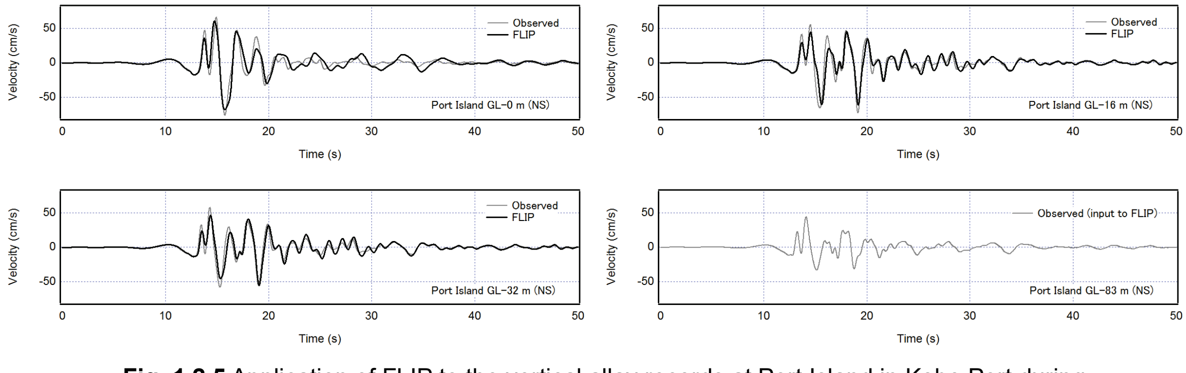

Fig. 1.2.5 Application of FLIP to the vertical allay records at Port Island in Kobe Port during the 1995 Hyogo-ken Nanbu earthquake[38]

③ **Numerical scheme**

Earthquake response analyses of the ground can be based on the multiple reflection theory, the finite element method, or other numerical schemes.

In the earthquake response analyses of the ground based on the multiple reflection theory, a horizontally layered ground is assumed as shown in **Fig. 1.2.6**. An incident shear wave, impinging vertically at the bedrock, is assumed to propagate upward, repeatedly causing reflection and transmission at the boundaries of the layers. The amplitudes of upcoming and downgoing waves in each layer are determined so that the boundary conditions are satisfied. Details of the formulation can be found in, for example, Osaki[25]. In the earthquake response analyses based on the multiple reflection theory, the soil can only be modelled as a linear or an equivalent linear material. Calculations are usually performed in the frequency domain. SHAKE[32], FDEL[35] and DYNEQ[36], among other programs, are based on the multiple reflection theory.

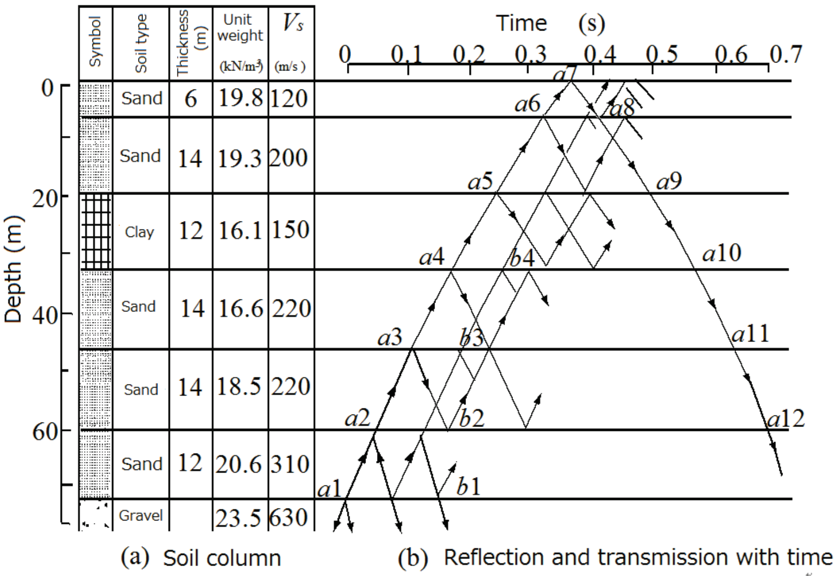

Fig. 1.2.6 Multiple reflection theory[23]

In the earthquake response analyses of the ground based on the finite element method, the ground is divided into a finite number of elements as shown in **Fig. 1.2.7** and the solution to the governing equation is obtained by replacing it with an algebraic equation in terms of displacements at nodal points. Obviously the application of the finite element method is not limited to geotechnical problems. The main advantage of the method is that it can be applicable to a ground with two or three dimensional variations in layer thickness and material properties. FLUSH[33] and FLIP[37], among other programs, are based on the finite element method. Calculations are performed either in the frequency domain or in the time domain, depending on the program.

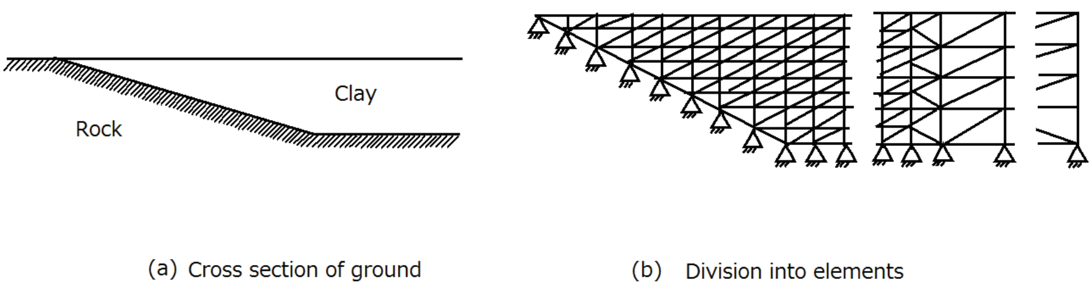

Fig. 1.2.7 Finite element method

(2) Modelling of the ground for earthquake response analyses

In the following section, the process of modelling the ground and determining model parameters will be described, with the emphasis on one dimensional analyses.

① **General**

To perform earthquake response analyses of the ground, the ground at a construction site should be divided into a stack of layers. Parameters such as the thickness, density and shear modulus at small strain are required for any kinds of analyses. In addition, for the equivalent linear analyses, the strain dependence of the shear modulus and damping factor should be specified. Parameters required for purely nonlinear analyses depend on how the stress-strain relation is modelled. In the case of FLIP, in addition to the above mentioned parameters, parameters such as the bulk modulus of the soil skeleton, the internal friction angle, the maximum damping factor and the parameters representing dilatancy should be specified. Among these parameters, the parameters representing dilatancy are only required for effective stress analyses.

② **Modelling procedure**

The engineering bedrock should be specified referring to the results of geotechnical investigations. There should be no significant difference in shear wave velocity between the layer regarded as the engineering bedrock in setting up design ground motions and the layer regarded as the engineering bedrock in the earthquake response analyses. The ground should be divided into a stack of layers, paying attention to the variation of soil type. Soils with different shear wave velocities, *SPT-N* values or q_u values should be assigned to different layers, even when the soil types are the same. Soils should be categorized into sand, clay or gravel. Actual soils are rarely composed of sand only or clay only. They are often combinations of gravel, sand, silt and clay with various percentages. Here, it is recommended that soils should be categorized as sandy soils if their fine fraction (<75μ) is less than 20%. Otherwise, soils should be regarded as clayey soils. Stones that constitute mounds and backfills should be regarded as gravels.

In terms of the density, observed values should be used if undisturbed samples are available and their densities are known. If those values are not available, the values listed in **Table 1.2.1** can conveniently be used. It should be noted that the values listed in **Table 1.2.1** are only suitable for earthquake response analyses; they are not suitable for other analyses where the density can be a decisive factor.

Table 1.2.1 Typical values of density[40)]

Soil type	Condition	Density (g/cm^3)
Clayey soil	Water content ≧60%	1.5
	Water content <60%	1.7
Sandy soil	Above water table	1.8
	Below water table	2.0
Mound / Backfill		2.0

The shear modulus at small strain (≈10^{-6}) can be determined from a shear wave velocity based on a PS logging as follows:

$$G_0 = \rho V_S^2 , \tag{1.2.3}$$

where

G_0 : Shear modulus at small strain

ρ : Density

V_S : Shear wave velocity

If PS logging data is not available for a sandy soil, the following equation can be used to estimate the shear modulus at small strain from an *SPT-N* value:

$$G_0 = 14100 N^{0.68} \quad (\text{kN/m}^2). \tag{1.2.4}$$

It should be noted that the equation shows an averaged relation derived from data with significant scattering[41]. For details, see also **Part II, Chapter 3, 2.4.1(6) Simplified evaluation of shear modulus and damping factor**.

For clayey soils, the following equation can be used to estimate the shear modulus at small strain from a q_u value obtained in an unconfined compression test:

$$G_0 = 170 q_u \,. \tag{1.2.5}$$

In estimating the shear wave velocity of a soil which will be overlain by a caisson, for example, using an *SPT-N* value, if the *SPT-N* value is available only before construction, the *SPT-N* value after construction can be estimated considering the increase in the effective overburden pressure due to a caisson or a mound.

$$N = \frac{(0.0041\sigma_v' + 0.7355)N_0 + 0.019(\sigma_v' - \sigma_{v0}')^B}{0.0041\sigma_{v0}' + 0.7355} \,, \tag{1.2.6}$$

where

N : *SPT-N* value after construction

N_0 : *SPT-N* value before construction

σ_v' : Effective overburden pressure after construction (kN/m^2)

σ_{v0}' : Effective overburden pressure before construction (kN/m^2)

If a soil will be subject to a change in the effective overburden pressure due to construction and PS logging data is only available before construction, the shear wave velocity after construction can be estimated from the shear wave velocity before construction considering the change in the effective overburden pressure using the following equation.

$$V_S = V_{S0}\left(\frac{\sigma_v'}{\sigma_{v0}'}\right)^B \,, \tag{1.2.7}$$

where

V_S : Shear wave velocity after construction

V_{S0} : Shear wave velocity before construction

σ_v' : Effective overburden pressure after construction (kN/m^2)

σ_{v0}' : Effective overburden pressure before construction (kN/m^2)

The value B can be 0.25 for a sandy soil or a clayey soil with I_p<30. It can be 0.5 for a clayey soil with $I_p \geqq 30$.

Less information is available regarding the shear wave velocities of a gravel mound or a gravel backfill because it is difficult to measure those quantities in-situ. For the shear wave velocities of a gravel mound or a gravel backfill of a large quay wall with the depth of approximately 10 m, the following values, estimated from an equation[42] derived from the results of earthquake observations for a composite breakwater, can be used:

Shear wave velocity of a gravel mound: V_S=300 m/s

Shear wave velocity of a gravel backfill: V_S=225 m/s

On the other hand, in another application[43], the shear wave velocity of 300 m/s for an effective confining pressure of 98 kN/m^2 was assumed both for a gravel mound and a gravel backfill.

If a caisson is assumed as part of the ground, the following value can be used as the shear wave velocity of a caisson.

Shear wave velocity of a caisson: V_S=2000 m/s

It has been recognized that the shear modulus of a soil at small strain is proportional to some power of the effective confining pressure. Because the shear modulus and the shear wave velocity are related to each other through **equation (1.2.3)**, the above mentioned proportionality means that the shear wave velocity of a soil is proportional to some power of the effective confining pressure.

According to existing element test results[26)44)], the proportionality can be given as follows:

(a) For a clayey soil with $I_p \geqq 30$, the shear modulus is proportional to the effective confining pressure.

(b) For a sandy soil or a clayey soil with $I_p<30$, the shear modulus is proportional to the effective confining pressure to the power of 0.5.

On the other hand, **Fig. 1.2.8** shows the result of a centrifuge test where centrifugal acceleration ranging from 10 G to 50 G was applied to a 24 cm thick ground with Toyoura sand to artificially vary the effective confining pressure[45)]. Fig. **1.2.8** shows the averaged shear wave velocity versus the effective confining pressure at the center of the sand layer. Fitted lines in the form of $V_S=K(\sigma_c')^a$ are also plotted. The averaged shear wave velocity increased with the increase of the centrifugal acceleration, indicating the dependence on the confining pressure. **Fig. 1.2.9** shows the shear wave velocity profiles estimated for the same specimens. The dotted lines indicate the curves with the assumption that the shear wave velocity is proportional to the effective confining pressure to the power of 0.25. Those curves were plotted so that they approach to the observed values for the central layer. For both cases, the shear wave velocity increased with depth and its dependence can be explained well with the assumption that the shear wave velocity is proportional to the effective confining pressure to the power of 0.25.

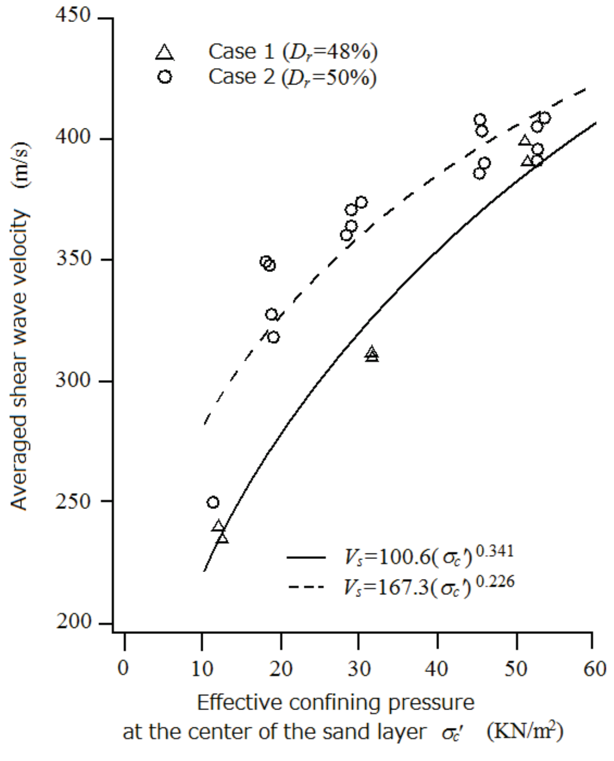

Fig. 1.2.8 Averaged shear wave velocity for a sand layer versus the effective confining pressure[45)]

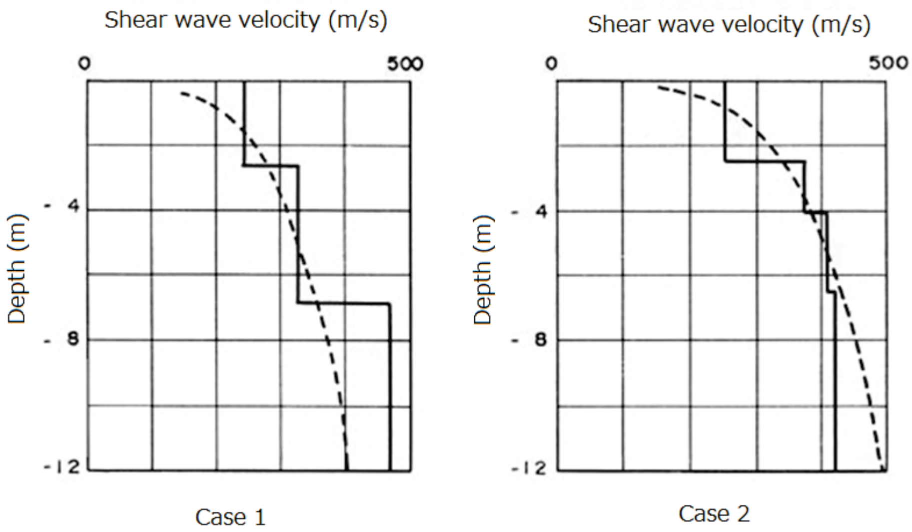

Fig. 1.2.9 Shear wave velocity profiles[45)]

③ **Strain dependence of shear modulus and damping factor**

In general, the shear modulus is large and the damping factor is small at small strain. With the increase in strain, the former decreases and the latter increases (**Fig. 2.4.2** in **Part II, Chapter 3, 2.4.1 Parameters for dynamic deformation**). The strain dependence of the shear modulus and damping factor could be dependent on the soil types and the confining pressure. Therefore, it is recommended to use strain dependent shear moduli and damping factors based on laboratory tests.

④ **Parameters for purely nonlinear analyses**

See Reference (Part III), Chapter 1, 2 Basic points of seismic response analyses for the determination of parameters for purely nonlinear analyses.

1.2.4 Correction of level-1 ground motions

If the site amplification factor that was used to calculate the existing level-1 ground motion available at the website of the National Institute for Land and Infrastructure Management at http://www.ysk.nilim.go.jp/kakubu/kouwan/sisetu/sisetu.html is not equivalent to the site amplification factor at a construction site, it is necessary to use the newly evaluated site amplification factor at the construction site by means of earthquake observations (See **Part II, Chapter 6, 1.2.2 Evaluation of site amplification factors (1)**) and/or microtremor measurements (See **Part II, Chapter 6, 1.2.2 Evaluation of site amplification factors (2)**) and to correct the existing level-1 ground motion before it is used for the design. The procedure can be as follows:

First, the existing level-1 ground motion at the engineering bedrock (a) should be obtained and transformed to an acceleration Fourier spectrum (b). Then, the site amplification factor at the same site at the engineering bedrock with respect to the seismological bedrock (c) should be obtained. By dividing (b) with (c), the acceleration Fourier spectrum of the level-1 ground motion at the seismological bedrock (d) can be obtained. Both (a) and (c) can be downloaded from the above mentioned website.

Then, the acceleration Fourier spectrum of the level-1 ground motion at the seismological bedrock (d) should be multiplied by the newly evaluated site amplification factor at the construction site at the engineering bedrock with respect to the seismological bedrock to obtain the acceleration Fourier spectrum of the level-1 ground motion at the construction site at the engineering bedrock.

Regarding waveform data to determine the phase characteristics of the level-1 ground motion, it is preferable to select the data from weak motion records at the construction site to take into account regional characteristics if the site amplification factor at the construction site has been evaluated by means of earthquake observations. If multiple weak motion records are available, it is preferable to select a record with average group delay time. The selected weak motion data should be converted to a “2E wave” at the engineering bedrock using geotechnical data at the site of earthquake observations and its phase characteristics should be used. If the site amplification factor at the construction site has been evaluated by means of microtremor measurements, the phase characteristics of the original level-1 ground motion can be used.

The acceleration time history of the level-1 ground motion at the engineering bedrock can be evaluated by combining the acceleration Fourier spectrum of the level-1 ground motion at the engineering bedrock with the phase characteristics mentioned above and applying the inverse Fourier transform.

1.3 Level-2 ground motions for the performance verification of structures

1.3.1 General

Level-2 ground motions can be defined as the ground motion with greatest intensity among anticipated ground motions at a construction site. In general, Level-2 ground motions are determined based on strong motion simulations, taking into account the source and path effects and the site amplification factor at the engineering bedrock with respect to the seismological bedrock. Level-2 ground motions can be regarded as the “reference earthquake motions for safety during or after an earthquake” in ISO23469[31)]. The concept of “safety” in ISO23469 involves the ability for a critical facility to be operational for post-earthquake emergency transportation. Therefore, “safety” in ISO23469 has a slightly broader meaning than “safety” in **Part I, Chapter 1, 3.7 Performance requirements**. The ground motions to be determined are the so called “2E wave”[23)], which is the incident wave impinging at the surface of the engineering bedrock multiplied by 2. The procedure to determine level-2 ground motions can be as follows (**Fig. 1.3.1**):

① Selection of scenario earthquakes (**Part II, Chapter6, 1.3.2**)

② Determination of source parameters (**Part II, Chapter6, 1.3.3**)

③ Evaluation of site amplification factors (**Part II, Chapter6, 1.3.4**)

④ Simulation of strong ground motions (**Part II, Chapter6, 1.3.5**)

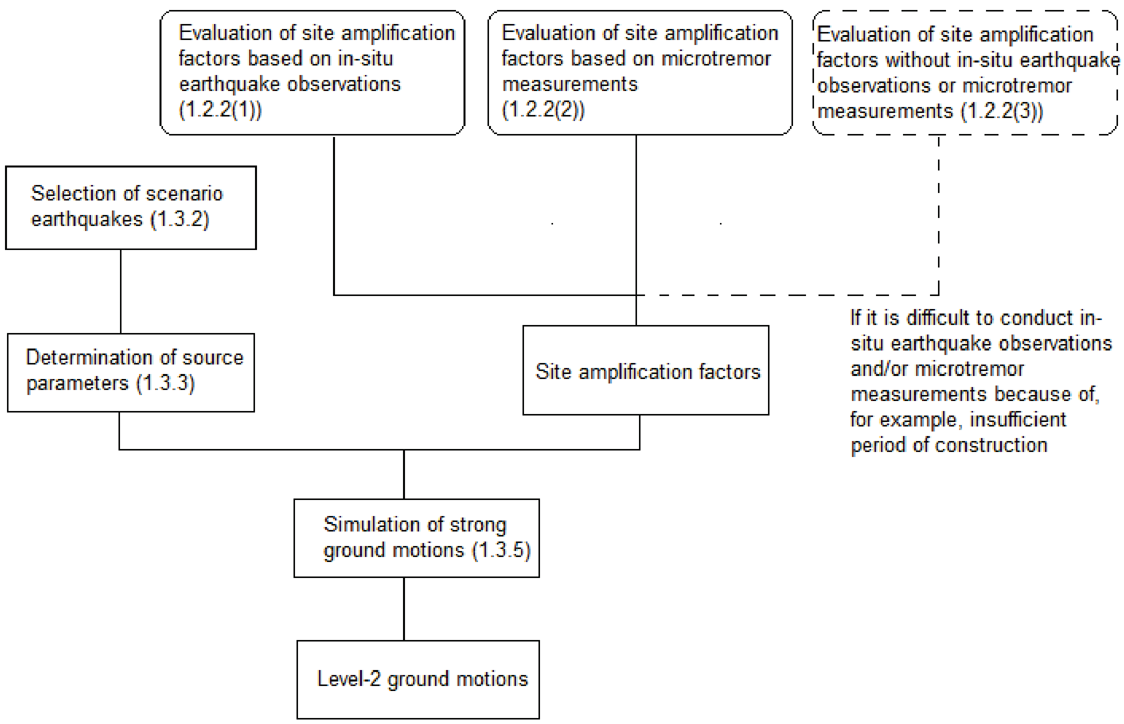

Fig. 1.3.1 Procedure to determine level-2 ground motions

It is desirable to evaluate the site amplification factor at a construction site by means of earthquake observations (See **Part II, Chapter 6, 1.2.2 Evaluation of site amplification factors (1)**). The site amplification factor at the construction site can also be evaluated by means of microtremor measurements (See **Part II, Chapter 6, 1.2.2**

Evaluation of site amplification factors (2)), however, it should be noted that uncertainties are inherent in the evaluation of site amplification factors based on microtremor measurements.

If it is difficult to conduct in-situ earthquake observations and/or microtremor measurements because of, for example, insufficient period of construction, the site amplification factor at the construction site can be evaluated by using an empirical relation (See **Part II, Chapter 6, "1.2.2 Evaluation of site amplification factors (3)**) based on a site amplification factor at a nearby strong motion station. In that case, it is important to recognize that the accuracy of the ground motions will be significantly degraded compared to cases with site amplification factors based on earthquake observations and/or microtremor measurements.

The ground motion evaluated through the following procedure can be different from that evaluated by another organization for a similar earthquake scenario primarily because of the difference of the ways in which the site effects are evaluated. If the ground motion is to be evaluated for the performance verification of a port structure, the following procedure can be followed.

For the detailed procedures of the performance verification of a structure, see the descriptions in **Part III** depending on the type of the structure.

1.3.2 Selection of scenario earthquakes

In selecting scenario earthquakes to determine Level-2 ground motions, it is necessary to comprehensively consider information regarding past earthquakes and active faults. In particular, it is necessary to consider the latest information regarding active faults at the time of the performance verification of a facility. Chronological Scientific Tables[46)] and Materials for Comprehensive List of Destructive Earthquakes in Japan[47)] can be suggested as comprehensive documents regarding past earthquakes in Japan. Handbook of Earthquake Fault Parameters in Japan[48)] can be suggested as a comprehensive document regarding fault parameters of past major earthquakes in Japan. Active Faults in Japan[49)] and Digital Active Fault Map of Japan[50)] can be suggested as comprehensive documents regarding active faults in Japan. In addition to these documents, after the 1995 Hyogo-ken Nanbu earthquake, surveys on active faults have been actively conducted in Japan and their results have been published from the Headquarters for Earthquake Research Promotion or local governments. On the bases of those documents, following earthquakes should be considered.

(a) Recurrence of past damaging earthquakes

(b) Earthquakes caused by active faults

(c) Other earthquakes expected from seismological and/or geological point of view

(d) Scenario earthquakes hypothesized by government agencies such as the Central Disaster Management Council and the Headquarters for Earthquake Research Promotion

(e) Scenario earthquakes hypothesized by local governments

(f) M6.5 earthquake just beneath the site[1)]

Some of the earthquakes (a) – (f) could overlap each other. From these earthquakes, earthquakes that could result in ground motions with greatest intensity at the port should be selected as the scenario earthquakes for calculating level-2 ground motions. However, it is sometimes difficult to decide which of these earthquakes could bring ground motions with greatest intensity at the port, especially when a smaller earthquake at a smaller distance and a greater earthquake at a greater distance are anticipated. In addition, because there are various aspects in ground motions such as amplitude, frequency content and duration, sometimes we can know which earthquake has the biggest effect on a facility only after ground motion simulations and earthquake response analyses are completed. Therefore, it is not reasonable to try to select only one earthquake at the initial stage. It is more reasonable to select multiple candidate earthquakes. In that case, among candidate level-2 ground motions, the ground motion that turns out to have the biggest effect on a facility as a result of earthquake response analyses should eventually be defined as the level-2 ground motion. If there are too many candidate earthquakes, a simple ground motion prediction equation can be used to reject earthquakes with obviously small effects. Regarding earthquakes in (d), the following websites are informative:

Central Disaster Management Council, Japan: http://www.bousai.go.jp/kaigirep/chuobou/senmon/index.html

Headquarters for Earthquake Research Promotion, Japan: http://www.jishin.go.jp/main/p_hyoka02.htm

An M6.5 earthquake just beneath the site is considered for the following reasons[1)]: While active faults can be defined as the signs of surface fault traces of past earthquakes, surface fault traces do not appear for a relatively small earthquake, indicating that relatively small earthquakes can occur in a region without known active faults. Takemura[51)] investigated the relation among the size of an earthquake, the frequency of the appearance of a surface fault trace and the damage rank[52] for M≧5.8 crustal earthquakes in 1885 – 1995 in Japan (**Fig. 1.3.2**). He found that, while M≦6.5 earthquakes seldom accompany surface fault traces, M≧6.8 earthquakes almost always accompany surface fault traces. He also noticed that there have been fewer earthquakes with M6.6 and M6.7 and suggested that, once an earthquake that could potentially be an M6.6 or M6.7 earthquake is initiated, it will break the shallower part of the crust, resulting in an M≧6.8 earthquake. Based on these reports, it has been suggested that an M6.5 earthquake is suitable as a scenario earthquake in a region without known active faults.

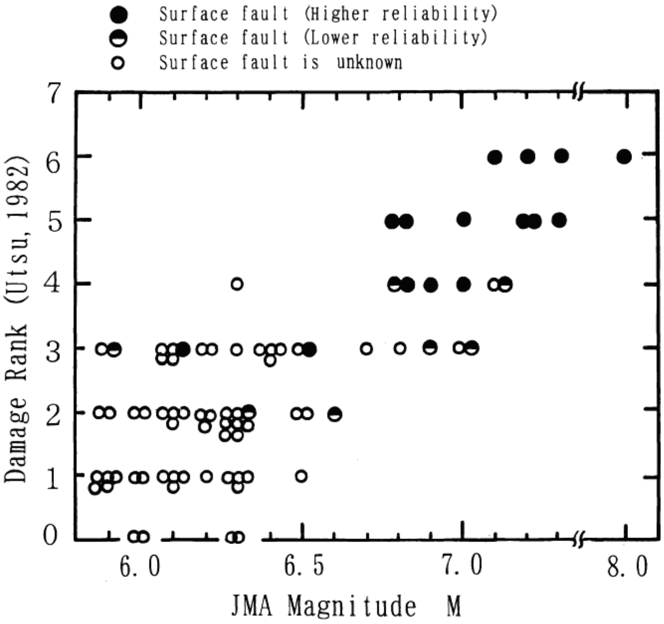

Fig. 1.3.2 Relation between the size of an earthquake and the frequency of the appearance of a surface fault trace[51]

If a design tsunami and its preceding ground motion is to be specified and the performance of a structure is to be verified for this combination, the preceding ground motion could be different from a level-2 ground motion. Let us assume that an inland crustal earthquake and a subduction earthquake are anticipated at a port and the former is anticipated to result in a more intense ground motion. In this situation, it is not reasonable from an economic point of view to combine the former ground motion with a tsunami, because the inland crustal earthquake will not accompany a tsunami; a level-2 ground motion and a ground motion preceding a tsunami should be specified separately. The procedure to determine a level-2 ground motion, which will be described below, can be applied to determining a ground motion preceding a tsunami by replacing the scenario earthquake.

1.3.3 Determination of source parameters

The source parameters to be determined fall into three categories: the outer parameters, the inner parameters and additional parameters. The outer source parameters include the location of the fault, the strike of the fault, the dip of the fault, the length of the fault, the width of the fault and the seismic moment of the fault. The inner source parameters include the number of the asperities, the area of the asperities, the seismic moment of the asperities and the rise time of the asperities. The additional parameters include the rupture starting point, the rupture velocity and the rupture propagation pattern. The meanings of the source parameters are shown in **Fig. 1.3.3**. The source parameters should be determined either based on the standard procedure described below or based on independent detailed surveys.

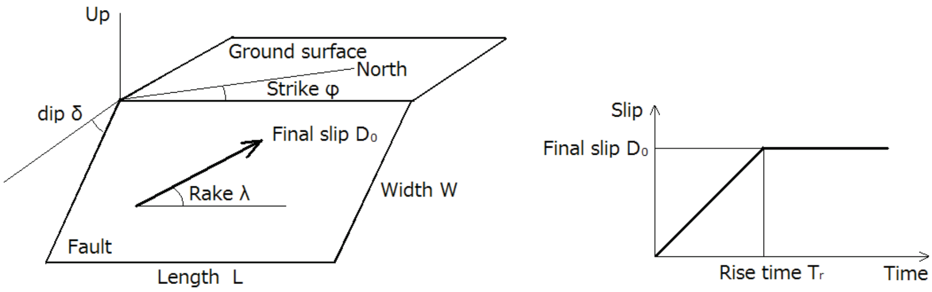

Fig. 1.3.3 Meanings of the source parameters

(1) Recurrence of past damaging earthquakes

If the recurrence of a past damaging earthquake is considered, it is preferable to effectively use the data regarding that particular past event, especially when a subduction earthquake is considered.

In terms of outer source parameters, the parameters for the past event can be used if they are known. Handbook of Earthquake Fault Parameters in Japan[48] provides information regarding outer source parameters for past earthquakes. If one of the two outer parameters, namely, the seismic moment M_0 and the area of the fault S is known and the other is to be estimated, **equation (1.3.1)**[53)54)] can be used:

$$S(\mathrm{km}^2) = 1.88 \times 10^{-15} \times M_0{}^{2/3}(\mathrm{dyne} \cdot \mathrm{cm}) \, . \qquad \textbf{(1.3.1)}$$

Equation (1.3.1) implies that the average stress drop on the fault is 3 MPa once the equation is combined with Esherby's equation for a circular crack[55)].

In terms of the inner source parameters such as the location of the asperities, different strategies are required depending on the availability of the data. Inner source parameters of a past event can be used if they have been sufficiently studied based on waveform data. This applies for a case of considering the recurrence of the 1968 Tokachi-oki earthquake[38)] (M7.9) or the 1978 Miyagi-ken-oki earthquake[38)] (M7.4). For a past event for which waveform data is not available, if seismic intensity data is available based on historical documents, inner source parameters that have been determined to be consistent with the data can be used.

The additional source parameters such as the rupture starting point can be determined in a similar way as the inner source parameters.

When earthquakes caused by active faults are considered, it is generally difficult to rely on waveform data or seismic intensity data for a past event because recurrence intervals are generally long for earthquakes caused by active faults. As an exception to this, if the recurrence of the 1995 Hyogo-ken Nanbu earthquake is considered, the above idea can be applied, instead of the procedure described in **(2) Earthquakes caused by active faults**.

When subduction earthquakes are considered, the SPGA model can be used to fit to waveform data or seismic intensity data. As an example of the SPGA model, **Fig. 1.3.4** shows the SPGA model that was used to explain the waveform data of the 2011 Tohoku earthquake (M_w9.0)[12)13)56)57)].

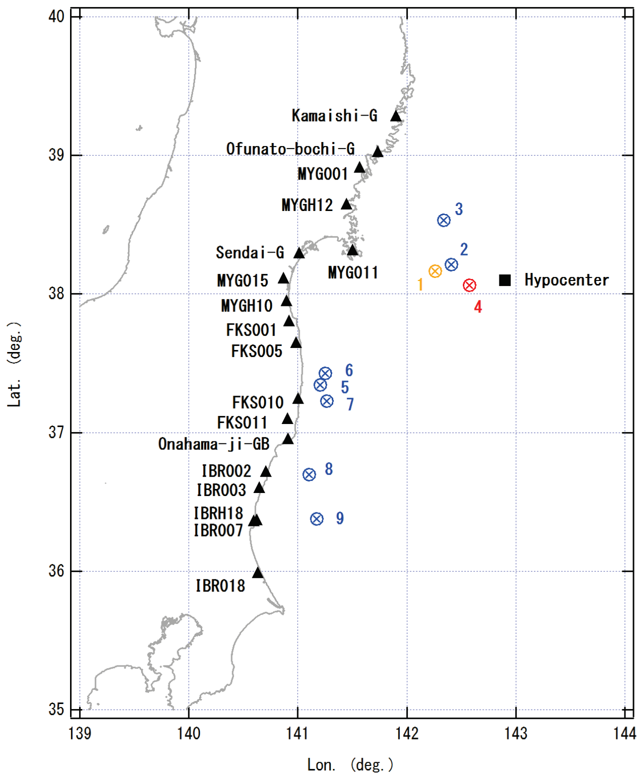

Fig. 1.3.4 SPGA model for the 2011 Tohoku earthquake[12)13)56)57)]

(2) Earthquakes caused by active faults

The outer source parameters of an earthquake caused by an active fault can be determined as follows: Based on geological and/or geomorphological investigations, the strike ϕ and dip δ of the fault should be determined. At the same time, the length of the fault or its segment should be determined and denoted as L. The dip δ can be 90°, 60°, 30° and 45° for a strike-slip fault, a high-angle reverse fault, a low-angle reverse fault and a reverse fault with no information on the dip angle, respectively, if there is no specific information to determine the dip angle. Because the fault width W of an earthquake caused by an active fault is restricted by the thickness H of the seismogenic layer in the upper crust, W can be determined by the following equation: $W=L$ if $L<H/\sin\delta$ and $W=H/\sin\delta$ if $L>H/\sin\delta$[54)58)]. The thickness of the seismogenic layer can be 20 km if there is no specific information to determine the thickness. The area of the fault S can be determined as the product of the length L and the width W. The seismic moment M_0 can be determined from the area of the fault S by using the following empirical relation[59)]:

$$S(\mathrm{km}^2) = 2.23 \times 10^{-15} \times M_0^{\ 2/3}(\mathrm{dyne \cdot cm}) \,. \tag{1.3.2}$$

The inner source parameters of an earthquake caused by an active fault can be determined as follows: If an earthquake that involves the rupture of multiple faults or multiple fault segments is considered, the following procedure can be applied to each of the faults or fault segments. The combined area of the asperities can be 22% of the fault area[54)58)59)60)61)]. Generally one or two asperities are considered[54)]. If an earthquake of M≧7.0 is considered, generally two asperities are considered. If two asperities are considered, the areas of the asperities can be 16% and 6% of the fault area for the larger and smaller of the asperities, respectively[54)60)]. It is preferable to consider square asperities whenever possible[54)59)]. The combined moment of the asperities can be 44% of the total moment of the earthquake[54)59)60)]. If two asperities are considered, the moments of the asperities can be 36% and 8% of the total moment of the earthquake for the larger and smaller of the asperities, respectively[54)60)]. The rise time τ of an asperity can be determined from the width of the asperity W_a and the rupture velocity V_r with the following equation:

$$\tau = \left(W_a / V_r\right) / 4 \,. \tag{1.3.3}$$

The locations of the asperities, together with the location of the rupture starting point, should be determined so that the rupture of one of the asperities propagates toward the port. This recommendation is based on the fact that especially intense ground motions are generally generated in the direction of the rupture propagation of an asperity and that the significant damage during the 1995 Hyogo-ken Nanbu earthquake was partly caused by this effect[4)]. The locations of the asperities can be determined referring to **Fig. 1.3.5**. The depth of the asperity center can be 10 km. If two asperities are considered, it is preferable to avoid concentrating two asperities on one side of the fault.

Among the additional parameters, the rupture starting point can be determined referring to **Fig. 1.3.5**, together with the locations of the asperities. The rupture velocity can be 80% of the shear wave velocity in the source region[54)]. The rupture can be assumed to propagate radially.

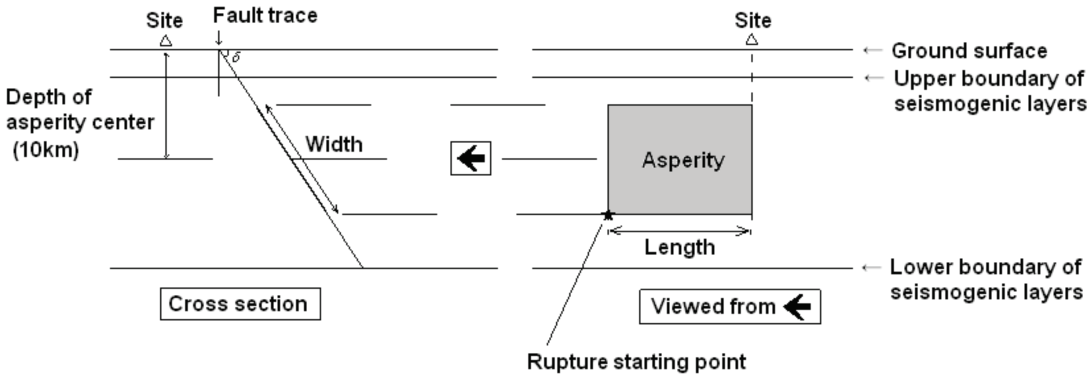

Fig. 1.3.5 Location of the asperity and the rupture starting point

(3) Huge subduction earthquakes greater than regional historical earthquakes

The occurrence of the 2011 Tohoku earthquake encouraged engineers to consider huge subduction earthquakes greater than regional historical earthquakes in various regions in Japan. In that case, the SPGA model[12)13)56)57)], which shows excellent applicability to past huge subduction earthquakes including the 2011 Tohoku earthquake, can be used. If a huge subduction earthquake comparable to the 2011 Tohoku earthquake is considered, the inner source parameters of the SPGA model can be determined referring to the inner source parameters of the SPGA model for the 2011 Tohoku earthquake[62)63)] (**Fig. 1.3.4**). If a huge subduction earthquake with a different size is considered, the inner source parameters of the SPGA model can be determined based on empirical relations[12)13)]. When a huge subduction earthquake greater than regional historical earthquakes is considered, the locations of the SPGAs cannot be constrained by seismic intensity data of historical earthquakes, leading to uncertainty in the locations of the SPGAs. Therefore, a lot of possible distributions of the SPGAs should be considered before selecting the locations[62)63)]. For example, if a huge subduction earthquake along the Nankai trough with M_w9.0 is considered, among possible distributions of the SPGAs, it is reasonable to select a distribution that generates ground motions that are consistent on average with the seismic intensity distributions anticipated by the Cabinet Office[64)]. Seismic intensity distributions calculated by SPGA models and those anticipated by the Cabinet Office were compared by Nozu et al.[65)].

(4) M6.5 earthquake just beneath the site

The seismic moment M_0 can be determined from the magnitude M with the following empirical relation[66)]:

$$\log M_0 = 1.17M + 17.72(\text{dyne}\cdot\text{cm}). \tag{1.3.4}$$

The area of the fault S can be determined with **equation (1.3.2)**. The dip δ can be 90°. Then, the procedure described in **(2) Earthquakes caused by active faults** can be followed. Generally one asperity is considered.

1.3.4 Evaluation of site amplification factors

The site amplification factor at a construction site can be evaluated in a similar way as in the case of a level-1 ground motion as described in **Part II, Chapter 6, 1.2.2 Evaluation of site amplification factors**.

1.3.5 Simulation of strong ground motions

(1) General

Methods for the simulation of strong ground motions taking into account the source, path and site effects can be broadly categorized into theoretical methods and semi-empirical methods. In the theoretical methods, the media through which seismic waves are transmitted from the source to a port is modelled as an elastic body and the ground motions are calculated by solving elastic wave equations. In the empirical Green's function method[67)68)69)], which is one of the semi-empirical methods, a recorded ground motion of a small event that shares the focal mechanism, that is, the strike, dip and rake angles and the propagation path with the anticipated large event is regarded as a Green's function and superposed to estimate the ground motion of the large event. In the stochastic Green's function method[70)], which is also one of the semi-empirical methods, the ground motion of a small event is artificially generated and superposed. This method is applicable when there is no appropriate record of a small event. In addition to these methods, hybrid methods (*e.g.*, Kamae et al[71)]) have also been proposed, in which low frequency components are calculated with a theoretical method and high frequency components are calculated with a semi-empirical method.

Among these methods, it has been shown that the theoretical methods can reproduce observed ground motions with high accuracy for frequencies lower than 1 Hz if they are applied to regions with sufficient information on subsurface structures (*e.g.*, Matsushima and Kawase[72)]). However, regions with sufficient information are quite limited in spite of efforts to collect information on subsurface structures (*e.g.*, Science and Technology Agency[73)]). On the other hand, in the empirical Green's function method that belongs to the semi-empirical methods, the site effects included in the Green's function will be naturally imposed on the results. In addition, within the framework of the stochastic Green's function method that belongs to the semi-empirical methods, it is possible to incorporate site amplification factors evaluated based on earthquake observations[38)74)]. This method will be referred to as the "corrected empirical Green's function method" in this article. In conclusion, in Japanese ports where strong motion records have been accumulated, it is preferable to use semi-empirical methods for the simulation of strong ground motions. In regions with sufficient information on subsurface structures, it is possible to use theoretical methods or hybrid methods, however, it is necessary to validate the appropriateness of the subsurface structure models using strong motion records before they are used.

It is meaningful to compare the results of strong motion simulations with strong motion records obtained in a similar condition. Comparing the results of strong motion simulations at a near-fault site of a crustal earthquake with, for example, near-fault records of the 1995 Hyogo-ken Nanbu earthquake or the 2004 Mid Niigata Prefecture earthquake will give some indications on the appropriateness of the results. However, because strong ground motions are strongly dependent on the source and site effects, the amplitude of a simulated ground motion can be different from those of past strong motion records depending on calculation conditions. If the amplitude of a simulated ground motion is significantly different from those of past strong motion records, it is preferable to investigate whether it is possible to reasonably explain the difference by considering the difference of the source and/or site effects. If it is possible, the result is acceptable. If it is not possible, it is necessary to check for mistakes in the input files, etc. Thus, comparison with past strong motion records is meaningful for preventing mistakes.

In comparing the results of strong motion simulations with past strong motion records, it is less meaningful to compare them in terms of peak ground accelerations. While peak ground accelerations are mostly affected by frequency components higher than 2 Hz, port facilities are less affected by frequency components higher than 2 Hz. Therefore, comparison in terms of peak ground accelerations does not make it possible to validate simulated ground motions in a frequency range that affects port facilities. In general, peak ground velocities are better indices than peak ground accelerations. Peak ground velocities in a range of 100 – 150 cm/s were observed at near-fault strong motion stations at the ground surface in sedimentary basins during the 1995 Hyogo-ken Nanbu earthquake and the 2004 Mid Niigata Prefecture earthquake.

(2) Corrected empirical Green's function method[38)74)]

In the corrected empirical Green's function method, the ground motion of a small event at a construction site is evaluated and called a "Green's function". Then the Green's functions are superposed to estimate the ground motion of a large earthquake. The details are as follows.

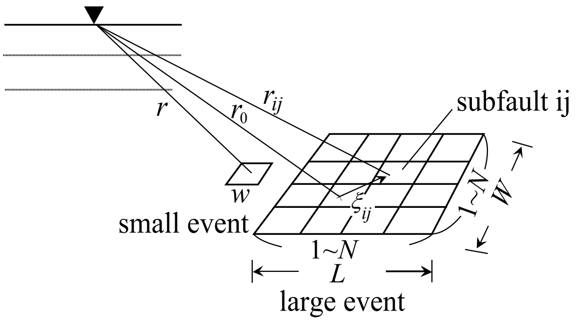

Fig. 1.3.6 Superposition of Green's functions. L and W are the length and width of an asperity, etc., respectively.

An asperity, etc. of a scenario earthquake is considered, which is shown as a "large event" in **Fig. 1.3.6**. The asperity is divided into $N \times N$ subfaults and a small earthquake that has the same area as one of the subfaults is considered, which is shown as a "small event" in **Fig. 1.3.6**. The Fourier amplitude spectrum of the Green's function at the ground surface is evaluated as the product of the source effect of the small event (**equation (1.3.5))**, the path effect (**equation (1.3.6)**) and the site amplification factor[75)]:

$$S(f) = R_{\theta\phi} FS \cdot PRTITN \cdot \frac{M_{0e}}{4\pi\rho V_S^3} \frac{(2\pi f)^2}{1+(f/f_c)^2} \qquad \textbf{(1.3.5)}$$

$$P(f) = \frac{1}{r}\exp\left(-\pi f r / Q V_S\right), \qquad \textbf{(1.3.6)}$$

where

$S(f)$: Source effect

$P(f)$: Path effect

M_{0e} : Seismic *moment* of the small event

f_c : Corner *frequency* of the small event

ρ : Density in the *seismological* bedrock

V_S : Shear wave *velocity* in the seismological bedrock

$R_{\theta\phi}$: Radiation *coefficient*

FS : Coefficient *representing* amplification due to free surface (=2)

$PRTITN$: Coefficient representing partition of S wave energy into two horizontal components

r : hypocentral *distance* of the small event

Q : Quality factor

If an earthquake caused by an active fault is considered, values such as ρ=2.7 g/cm^3 and V_S=3.5 km/s can be used. For $R_{\theta\phi}$, 0.63 can be used, which corresponds to the averaged value over all directions. *PRTITN* can be 0.85 and 0.53 for the strike-normal and strike-parallel components, respectively, if an earthquake caused by an active fault is considered and the fault distance is less than 10 km. These suggestions are based on a report that, on average, the Fourier amplitude spectrum is approximately 1.6 times larger for the strike-normal component than for the strike-parallel component in the near-fault regions of large crustal earthquakes[8)]. *PRTITN* can be 0.71 for any horizontal component if a scenario earthquake other than those caused by active faults is considered or if the fault distance is greater than 10 km, with the assumption that S wave energy is equally distributed into two horizontal components. In any case, *PRTITN* should be determined in such a way that their squared sum is equal to 1.0. The standard values for *PRTITN* are listed in **Table 1.3.1**.

Table 1.3.1 Standard values for *PRTITN*

	Near-fault sites	Other sites
Subduction earthquakes	0.71	0.71
Earthquakes caused by active faults	0.85 (strike-normal component) 0.53 (strike-parallel component)	0.71
M6.5 earthquake just beneath the site	0.71	0.71

The seismic moment of the small event M_{0e} can be calculated by dividing the seismic moment of the asperity, etc. by N^3, where N is the number of discretization. The corner frequency of the small event f_c can be calculated by the following equation proposed by Brune[76)77)].

$$f_c = \frac{0.66V_S}{\sqrt{S_e}}, \tag{1.3.7}$$

where

S_e : Area of the small event

Equation (1.3.7) is identical to **equation (36)** in the paper written by Brune[76)]. Once **equation (1.3.7)** is combined with the equation for a circular crack by Esherby[55)], one obtains the well-known equation for expressing the corner frequency as a function of the seismic moment and the stress drop[75)]. In **equation (1.3.6)**, the quality factor should be determined appropriately taking into account regional characteristics. Quality factors estimated for different regions include: Q=114 $f^{0.92}$ for subduction earthquakes in eastern Japan[78)], Q=152 $f^{0.38}$ for subduction earthquakes in western Japan[78)], Q=166 $f^{0.76}$ for crustal earthquakes in eastern Japan[78)], Q=63.8 $f^{1.00}$ for crustal earthquakes in the Kansai Region[79)] and Q=104 $f^{0.63}$ for crustal earthquakes in Kagoshima and Kumamoto prefectures[80)].

The Green's function at the ground surface can be evaluated by combining the Fourier amplitude spectrum at the ground surface thus obtained with the phase characteristics of a weak motion record at the construction site or in its vicinity and applying the inverse Fourier transform[38)74)]. The procedure can be expressed as follows:

$$A(f) = S(f)P(f)G(f)\frac{O(f)}{|O(f)|_p}, \tag{1.3.8}$$

where

$A(f)$: Fourier transform of a Green's function at the ground surface (complex value)

$S(f)$: Source effect (real value)

$P(f)$: Path effect (real value)

$G(f)$: Site amplification factor at the ground surface with respect to the seismological bedrock (real value)

$O(f)$: Fourier transform of a weak motion record at a construction site or in its vicinity (complex value)

$|O(f)|_P$: Absolute value of $O(f)$, smoothed with a Parzen window with a band width of 0.05 Hz

It is preferable to use a weak motion record at a construction site with a similar incident angle to the scenario earthquake in **equation (1.3.8)** to consider the influence of sediments on the phase characteristics of earthquake ground motions more appropriately.

Before evaluating a Green's function at the ground surface with **equation (1.3.8)**, it is necessary to evaluate the site amplification factor $G(f)$. So far two approaches have been used to evaluate the site amplification factor: One approach is to isolate the "S wave portion" from an observed ground motion and to evaluate the site amplification factor for that portion[81)]. The other approach is to account not only for S waves but also for surface waves and to evaluate the site amplification factor based on Fourier spectra including the effects of later phases[17)]. Although both of these approaches are meaningful under certain conditions, the latter approach should be taken if it is intended to consider not only S waves but also surface waves in the simulation of strong ground motions. In particular, within the framework of the corrected empirical Green's function method, because the effects of S waves and surface waves are inseparably included in a weak motion record to determine the phase characteristics of a Green's function, it is necessary to consider the effects of both waves in evaluating the Fourier amplitude spectrum.

The ground motion generated by the asperity, etc. can be calculated by superposing Green's functions at the ground surface with the following equation (**Fig. 1.3.6**) [82)]. Through the process of the superposition, the forward directivity effects are considered, resulting in stronger predicted ground motions in the direction of rupture propagation:

$$U(t) = \sum_{i=1}^{N}\sum_{j=1}^{N}\left(r/r_{ij}\right) f(t) * u(t - t_{ij}) \tag{1.3.9}$$

$$f(t) = \delta(t) + \frac{1}{n'\left(1-\frac{1}{e}\right)} \sum_{k=1}^{(N-1)n'} \left[e^{-(k-1)/(N-1)/n'} \delta\left\{ t - \frac{(k-1)\tau}{(N-1)n'} \right\} \right] \tag{1.3.10}$$

$$t_{ij} = \frac{r_{ij} - r_0}{V_S} + \frac{\xi_{ij}}{V_r}, \tag{1.3.11}$$

where

$U(t)$: Ground motion generated by the asperity, etc.

$u(t)$: Green's function at the ground surface

$f(t)$: Correction function for the difference of slip velocity time functions for the large and small events

r : hypocentral distance of the small event

r_{ij} : Distance from the *ij* subfault to the site

N : Number of discretization (Fig. 1.3.6)

τ : Rise time

n' : Integer to remove artificial periodicity that appears in the process of superposition

r_0 : Distance from the rupture starting point of the asperity, etc. to the site

ξ_{ij} : Distance from the rupture starting point of the asperity, etc. to the *ij* subfault

V_S : Shear wave velocity in the seismological bedrock

V_r : Rupture velocity

When two or more asperities, etc. are considered, the above mentioned process should be repeated for all the asperities, etc. and the resultant waveforms should be superposed to obtain the level-2 ground motion at the ground surface. The obtained ground motion, however, corresponds to a virtual situation where the shallower sediments above the engineering bedrock exhibit linear behavior. Finally, the level-2 ground motion at the engineering bedrock in the form of so-called "2E wave" can be evaluated by conducting earthquake response analyses of the shallow sediments. Contributions from the background region, *i.e.*, the region on the fault outside the asperities, etc., can be neglected if the strong motion simulation is aimed at generating ground motions for the performance verification of a typical port structure.

It should be noted that the level-2 ground motion at the ground surface that appears in the above process is often overestimated because it does not include the possible effects of soil nonlinearity for the shallower sediments during a large earthquake. If a realistic level-2 ground motion at the ground surface is required, it is generally obtained by nonlinear response analyses of the shallower sediments in which the level-2 ground motion at the engineering bedrock is used as an input motion.

So far, it has been assumed that a Green's function at the ground surface is used in **equation (1.3.9)**. However, a Green's function at the engineering bedrock in the form of "2E wave" can also be used in **equation (1.3.9)**. In that case, the level-2 ground motion at the engineering bedrock in the form of "2E wave" can be directly obtained. However, in that case, the site amplification factor at the engineering bedrock with respect to the seismological bedrock should be used in **equation (1.3.8)** and the weak motion record at the construction site or in its vicinity should be converted to a "2E wave" at the engineering bedrock before used in **equation (1.3.8)**.

Nozu et al.[38] applied the above mentioned method to reproduce strong motion records during past large earthquakes. A FORTRAN program based on the method is available on a CD attached to their report[38] or at the PARI website at https://www.pari.go.jp/bsh/jbn-kzo/jbn-bsi/taisin/sourcemodel/somodel_program.html.

(3) Empirical Green's function method

The empirical Green's function method assumes the existence of a weak motion record at a given site that recorded a small earthquake that occurred near the fault of a scenario earthquake. If such a record is available, it can be superposed to estimate the ground motion of the scenario earthquake at the site. The weak motion record is called the "empirical Green's function". The main advantage of the method is that the ground motion can be estimated accurately without explicitly evaluating the path and site effects, because those effects are naturally included in the weak motion record. However, the method cannot be applied if such a record is not available. In addition, the method requires more skills compared to the corrected empirical Green's function method as mentioned below:

Equations (1.3.9) – **(1.3.11)** for the corrected empirical Green's function method can almost be used for superposing empirical Green's functions, with the exception that **equation (1.3.9)** should be replaced by the following equation[82] that includes the coefficient C to appropriately consider the characteristics of the small earthquake:

$$U(t) = \sum_{i=1}^{N} \sum_{j=1}^{N} \left(r/r_{ij} \right) f(t) * \left(Cu(t - t_{ij}) \right). \tag{1.3.12}$$

Parameters related to the superposition N and C should be determined so that

$$M_{0a} / M_{0e} = CN^3$$

$$S_a / S_e = N^2 \, , \tag{1.3.13}$$

where

M_{0a} : Seismic moment of the asperity, etc.

M_{0e} : Seismic moment of the small event

S_a : Area of the asperity, etc.

S_e : Area of the small event

Equation (1.3.13) implies that it is inevitable to carefully evaluate the parameters of the small event in the application of the empirical Green's function method. For the seismic moment of the small event M_{0e}, moment tensor solutions[83] such as those determined by the F-net of the National Research Institute for Earth Science and Disaster Resilience, Japan, can be referred. The area of the small event S_e can be determined from the corner frequency of the small event with **equation (1.3.7)**. The corner frequency of the small event can be determined by taking the spectral ratio of closely-located earthquakes with different size[2][84].

Another issue to be carefully considered in the application of the empirical Green's function method is how to handle radiation coefficients. Theoretically speaking, radiation coefficients are dependent on the azimuth and the take-off angle[83][85]. Therefore, a weak motion record at a construction site may correspond to a small radiation coefficient depending on the focal mechanism of the small event. In that case, superposing that record may lead to underestimation of the ground motion of a scenario earthquake. Thus, it is necessary to pay attention to the focal mechanism of the small event.

The points raised above imply that there are several issues to be carefully considered in the application of the empirical Green's function method, indicating that the empirical Green's function method requires more skills compared to the corrected empirical Green's function method.

1.3.6 Earthquake response analysis of the ground

Earthquake response analyses of the ground can be conducted referring to **Part II, Chapter 6, 1.2.3 Earthquake response analysis of the ground** with the exception that the analysis method should be selected carefully because the strain level tends to become large for a level-2 ground motion.

1.4 Spatial variation of earthquake ground motions for the performance verification of structures

(1) General

In designing a long or a large structure such as a buried pipeline or a submerged tunnel, one of the issues to be considered is that various parts of the structure will be subject to different ground motions.

"Spatial variation of earthquake ground motions" generally refers to lateral variation of earthquake ground motions. Spatial variation of earthquake ground motions can be induced by lateral variation in ground conditions, however, spatial variation of ground motions can be induced by other factors. When lateral variation in ground conditions is negligible, apparent propagation of seismic waves in a horizontal direction can cause phase difference of earthquake ground motions acting on various parts of a structure. In the following section, both of these issues will be addressed.

It should be noted that lateral variation of earthquake ground motions is not the only reason for the difference of earthquake ground motions acting on various parts of a structure. Structures with significant depth variation in the longitudinal direction such as submerged tunnels are more susceptible to vertical variation of earthquake ground motions, which should be appropriately taken into account in the design.

(2) If lateral variation in ground conditions is significant

Significant lateral variation in ground conditions within the dimension of a structure can cause spatial variation of earthquake ground motions. Therefore, lateral variation in ground conditions within the dimension of a structure should be evaluated appropriately. If it is significant, spatial variation of earthquake ground motions should be evaluated taking into account its effects. In this evaluation, it is preferable to consider the lateral variation not only in the shallower sediments but also in the deeper sediments below the engineering bedrock.

Spatial variation of earthquake ground motions induced by significant lateral variation in ground conditions can be most effectively evaluated by conducting array observations of earthquake ground motions and applying the method described in **Part II, Chapter 6, 1.3.5 Simulation of strong ground motions (2)** and **(3)** to evaluate strong ground motions at multiple locations. Numerical methods such as the finite element method or the finite difference method are also applicable if there is sufficient information on subsurface structures. If the method described in **Part II, Chapter 6, 1.3.5 Simulation of strong ground motions (2)** is to be used, care should be taken not to loose the physical meaning of the phase difference of predicted ground motions at multiple locations. The physical meaning of the phase difference could be lost when 1) random numbers are used for generating Green's functions[75)] and different random numbers are assigned to different locations or 2) when weak motion records used in **equation (1.3.8)** for different locations have been triggered independently and cannot be aligned on the same time axis. For the former situation, it would be effective to use the same random numbers for different locations.

(3) If lateral variation in ground conditions is not significant

If lateral variation in ground conditions is not significant, the above mentioned procedure can also be applied, however, a simpler procedure[31)] can be applied as follows:

When lateral variation in ground conditions is not significant, apparent propagation of seismic waves in a horizontal direction can be a major cause of the spatial variation of earthquake ground motions. The strain in the ground due to the apparent propagation of seismic waves $\varepsilon(\omega)$ is a function of the particle velocity $v(\omega)$ and the apparent propagation velocity of the seismic waves $c(\omega)$:

$$\varepsilon(\omega) = v(\omega)/c(\omega), \qquad \textbf{(1.4.1)}$$

where ω is the angular frequency.

Because $\varepsilon(\omega)$ is a decreasing function of $c(\omega)$ as can be seen in **equation (1.4.1)**, using a smaller value of $c(\omega)$ leads to a more conservative design of a structure. Although both surface waves and obliquely incident S waves can cause apparent propagation of seismic waves in a horizontal direction, the phase velocity of the surface waves is smaller than that of the S waves for any angular frequency ω. Among surface waves, either fundamental-mode Love waves or fundamental-mode Rayleigh waves travel with the smallest phase velocity for any angular frequency ω. Therefore, it is most conservative to use the smaller of the phase velocities of fundamental-mode Love waves and fundamental-mode Rayleigh waves for $c(\omega)$.

In general, the phase velocity of surface waves is frequency-dependent. For example, **Fig. 1.4.1** shows the frequency dependent phase velocities of Love waves in a waterfront area of Tokyo. The theoretical phase velocities (solid lines) were computed from the S-wave velocity structure model shown in **Table 1.4.1**. The solid rectangles in **Fig. 1.4.1** indicate the phase velocities obtained from array observations of earthquake ground motions at this particular site. The phase velocity of the fundamental-mode Love wave is approximately 400 m/s at the period of one second and approximately 750 m/s at the period of 3 seconds, indicating that the phase velocity is frequency dependent.

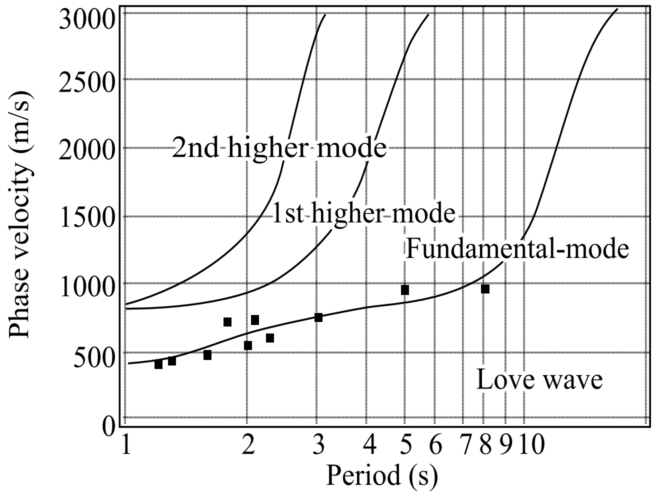

Fig. 1.4.1 Frequency dependent phase velocities of Love waves in a waterfront area of Tokyo[86)]

Table 1.4.1 S-wave velocity structure model [86)]

Thickness (m)	S wave velocity (m/s)	Density (10^3 kg/m^3)
50	250	1.8
120	410	1.9
1580	800	1.9
1250	1200	2.1
3100	2600	2.6
—	3400	2.6

The apparent velocity is significantly site-specific. The values shown in **Fig. 1.4.1** cannot be used at an arbitrary site. *The apparent velocity* for the performance verification of a structure should be determined on a site-specific basis.

Earthquake ground motions evaluated by the method described in **Part II, Chapter 6, 1.2 Level-1 ground motions for the performance verification of structures** or **Part II, Chapter 6, 1.3 Level-2 ground motions for the performance verification of structures** generally involve different types of seismic waves such as surface waves and S waves. Ideally speaking, $c(\omega)$ for the performance verification should be determined based on the knowledge of the types of waves involved in the evaluated ground motions. In practice, however, it is not easy to specify the types of waves. Therefore, the smaller of the phase velocities of fundamental-mode Love waves and fundamental-mode Rayleigh waves can be used for $c(\omega)$ if it is intended to be sufficiently conservative. The phase velocities should be determined through in-situ array observations of earthquake ground motions or microtremors (see **Reference (Part II), Chapter 1, 3.8.4 Array observations of microtremors**).

However, earthquake ground motions involve various types of seismic waves other than fundamental-mode surface waves. It is necessary to consider the effects of those waves if it is intended to evaluate the strain in the ground more realistically. From such a point of view, a study was conducted to determine a more realistic value of the apparent velocity based on the results of earthquake observations in a sealed tunnel[87)]. As a result, it was reported that the axial strain in the tunnel was well reproduced by assuming a seismic wave that travels with a velocity twice as large as the phase velocity of fundamental-model Love waves and intersects with the tunnel axis at 45°.

Considering a frequency dependent apparent velocity leads to a more rational design of a structure. However, a frequency independent apparent velocity is also used for simplicity. The apparent velocity along the tunnel axis obtained in the above mentioned study based on earthquake observations in a sealed tunnel[87] was slightly larger than a frequency independent apparent velocity of 1 km/s.

Spatial variation of earthquake ground motions can be evaluated with considerations of a frequency dependent *apparent velocity* as follows:

Let $a_0(t)$ denote the time history of a ground motion evaluated through the process described in **Part II, Chapter 6, 1.2 Level-1 ground motions for the performance verification of structures** or **1.3 Level-2 ground motions for the performance verification of structures** at one representative point (x=0, y=0) at a specified depth in a horizontally layered ground. Let $c(\omega)$ denote the site-specific frequency-dependent phase velocity. Then the ground motion $a(t)$ at an arbitrary point (x,y) at the same depth can be specified as follows:

① Compute the Fourier transform of $a_0(t)$.

② Compute the Fourier transform of $a(t)$ as follows:

$$A(\omega) = A_0(\omega)\exp\{-i(k_x x + k_y y)\} \tag{1.4.2}$$

$$k_x = \{\omega/c(\omega)\}\cos\theta \tag{1.4.3}$$

$$k_y = \{\omega/c(\omega)\}\sin\theta\,, \tag{1.4.4}$$

where

$A_0(\omega)$: Fourier transform of $a_0(t)$

$A(\omega)$: Fourier transform of $a(t)$

θ : Angle between the positive-*x direction and the propagation direction of the seismic wave*

③ Compute the inverse Fourier transform of $A(\omega)$ to obtain $a(t)$.

[References]

1) Japan Society of Civil Engineers: Proposal and commentary on seismic design standards for infrastructures: the third proposal, 2000 (in Japanese).

2) Aki, K.: Scaling law of seismic spectrum, J. Geophys. Res., Vol.72, pp.1217-1231, 1967.

3) Aki, K.: Generation and propagation of G waves from the Niigata earthquake of June 16, 1964. 2. Estimation of earthquake moment, released energy, and stress-strain drop from G wave spectrum, Bulletin of the Earthquake Research Institute, Vol.44, pp.23-88, 1966.

4) Irikura, K.: Near-fault ground motions causing the Great Hanshin Earthquake Disaster, Annuals, Disaster Prevention Research Institute, Kyoto University, No.39A, pp.229-245, 1996 (in Japanese with English abstract).

5) Koketsu, K.: Damaging earthquakes in California and the Hyogo-ken Nanbu earthquake, Kagaku, Vol.66, No.2, pp.93-97, 1996 (in Japanese with English abstract).

6) Takemura, M., T. Moroi and K. Yashiro: Characteristics of strong ground motions as deduced from spatial distribution of damages due to the destructive inland earthquakes from 1891 to 1995 in Japan, Zisin, 2nd series, Vol.50, pp.485-505, 1998 (in Japanese with English abstract).

7) Somerville, P.G., N.F. Smith, R.W. Graves and N.A. Abrahamson: Modification of empirical strong ground motion attenuation relations to include the amplitude and duration effects of rupture directivity, Seismological Research Letters, Vol.68, pp.199-222, 1997.

8) Nozu, A., S. Iai and W.D. Iwan: A study on predominant direction of near-source ground motion and its application, Report of the Port and Harbour Research Institute, Vol.40, No.1, pp.107-167, 2001 (in Japanese with English abstract)

9) Nozu, A. and K. Ikeda: Planning high seismic resistant quay walls with considerations of predominant direction of near-fault ground motions, Kowan, Vol.78, No.9, pp.48-51, 2001 (in Japanese).

10) Ports and Harbours Bureau, Ministry of Land, Infrastructure and Transport and Port and Airport Research Institute: Handbook of Predominant Direction of Earthquake Ground Motions for Port Planning, CD-ROM, 2003 (in Japanese).

11) Lay, T., H. Kanamori, C.J. Ammon, K.D. Koper, A.R. Hutko, L. Ye, H. Yue and T.M. Rushing: Depth-varying rupture properties of subduction zone megathrust faults, J. Geophys. Res., Vol.117, B04311, 2012.

12) Nozu, A., M. Yamada, T. Nagao and K. Irikura: Generation of strong motion pulses during huge subduction earthquakes and scaling of their generation areas, Journal of Japan Association for Earthquake Engineering, Vol.12, No.4, pp.209-228, 2012 (English translation is available in Vol.14, No.6).

13) Nozu, A. and T. Nagao: Strong motion pulse generation areas for huge subduction earthquakes: their scaling with overall earthquake size, Technical Note of the Port and Airport Research Institute, No.1257, 2012 (in Japanese with English abstract).

14) Kurahashi, S. and K. Irikura: Short-period source model of the 2011 M_w9.0 off the Pacific coast of Tohoku earthquake, Bull. Seism. Soc. Am., Vol.103, pp.1373-1393, 2013.

15) Street, R., R. Herrmann and O. Nuttli: Spectral characteristics of the L_g wave generated by central United States earthquakes, Geophys. J. R. Astr. Soc., Vol.41, pp.51-63, 1975.

16) Kudo, K.: Progress of engineering seismology in Japan, specially related with strong motion prediction: An introduction to the series of reviews on strong motion seismology and engineering seismology, Zisin, 2nd series, Vol.46, pp.151-159, 1993 (in Japanese with English abstract).

17) Nozu, A. and T. Nagao: Site amplification factors for strong-motion sites in Japan based on spectral inversion technique, Technical Note of the Port and Airport Research Institute, No.1112, 2005 (in Japanese with English abstract).

18) Kinoshita, S.: Kyoshin Net (K-net), Seim. Res. Lett., Vol. 69, pp.309-332, 1998.

19) Aoi, S., K. Obara, S. Hori, K. Kasahara and S. Okada: New strong-motion observation network: KiK-net, EOS, Trans. Am. Geophys. Union, Vol. 329, 2000.

20) Takemura, M.: Great Kanto Earthquake Disaster: Knowing Strong Ground Motions in Greater Tokyo, Kajima Institute Publishing, 2003 (in Japanese).

21) Nozu, A. and T. Sugano: Site amplification factors for strong-motion sites in Nansei Islands in Japan based on spectral inversion technique, Technical Note of the Port and Airport Research Institute, No.1149, 2007 (in Japanese with English abstract).

22) Nozu, A. and T. Sugano: Site amplification factors for strong-motion sites in Northern Hokkaido, Japan, based on spectral inversion technique, Technical Note of the Port and Airport Research Institute, No.1214, 2010 (in Japanese with English abstract).

23) Tsuchida, H. and S. Iai: Earthquake Engineering for Practitioners, Sankaido, 1991 (in Japanese).

24) Takenobu, M., A. Nozu, M. Miyata, Y. Sato and S. Asai: Comprehensive report for setting up level-1 earthquake ground motion with a probabilistic time history waveform for seismic design of port facilities, Technical Note of National Institute for Land and Infrastructure Management, No.812, 2014 (in Japanese with English abstract).

25) Osaki, Y.: Introduction to Spectral Analysis of Earthquake Ground Motions: New Edition, Kajima Institute Publishing, 2003 (in Japanese).

26) Zen, K., H. Yamazaki and Y. Umehara: Experimental study on shear modulus and damping ratio of natural deposits for seismic response analysis, Report of the Port and Harbour Research Institute, Vol.25, No.1, pp.41-113, 1987 (in Japanese with English abstract).

27) Nakamura, Y.: A method for dynamic characteristics estimation of subsurface layers using microtremor on the ground surface, Report of the Railway Technical Research institute, Vol.2, No.4, pp.18-27, 1988 (in Japanese with English abstract).

28) Nozu, A. and A. Wakai: Characteristics of ground motions at damaged ports during the 2011 Great East Japan Earthquake Disaster, Technical Note of the Port and Airport Research Institute, No.1244, 2011 (in Japanese with English abstract).

29) Nagao, T., N. Morishita and A. Nozu: Study on the effect of the site amplification factor on the evaluation of level-one earthquake ground motion, Proceedings of Civil Engineering in the Ocean, Vol.22, 2006 (in Japanese with English abstract).

30) Yoshida, N. and S. Iai: Nonlinear site response and its evaluation and prediction, The Effects of Surface Geology on Seismic Motion, Irikura, Kudo, Okada & Sasatani (eds), Balkema, 1998.

31) International Organization for Standardization: ISO23469, Bases for design of structures - Seismic actions for designing geotechnical works, 2005.

32) Shnabel, P.B., J. Lysmer and H.B. Seed: SHAKE, A computer program for earthquake response analysis of horizontally layered sites, Report No. EERC72-12, University of California at Berkeley, 1972.

33) Lysmer, J., T. Udaka, C.F. Tsai and H.B. Seed: FLUSH, A computer program of approximate 3-D analysis of soil-structure interaction problems, Report No. EERC75-30, University of California at Berkeley, 1975.

34) Yoshida, N.: Applicability of conventional computer code SHAKE to nonlinear problem, Proceedings of the Symposium on Amplification of Ground Shaking in Soft Ground, the Japan Society of Soil Mechanics and Foundation Engineering, Tokyo, pp.14-31, 1994 (in Japanese).

35) Sugito, M., H. Goda and T. Masuda: Frequency dependent equi-linearized technique for seismic response analysis of multi-layered ground, Journal of JSCE, No.493/III-27, pp.49-58, 1994 (in Japanese with English abstract).

36) Yoshida, N. and I. Suetomi: DYNEQ: A computer program for dynamic response analysis of level ground by equivalent linear method, Report of the Technical Institute, Sato Kogyo Co., Ltd., pp.61-70, 1996 (in Japanese).

37) Iai, S., Y. Matsunaga and T. Kameoka: Strain space plasticity model for cyclic mobility, Soils and Foundations, Vol.32, pp.1-15, 1992.

38) Nozu, A. and T. Sugano: Simulation of strong ground motions based on site-specific amplification and phase characteristics – Accounting for causality and multiple nonlinear effects –, Technical Note of the Port and Airport Research Institute, No.1173, 2008 (in Japanese with English abstract).

39) Iai, S., T. Morita, T. Kameoka, Y. Matsunaga and K. Abiko: Response of a dense sand deposit during 1993 Kushiro Oki earthquake, Soils and Foundations, Vol.35, pp.115-132, 1995.

40) Coastal Development Institute of Technology: Handbook on Liquefaction Remediation of Reclaimed Land, Revised Edition, 1997 (in Japanese).

41) Imai, T. and K. Tonouchi: Correlation of N value with S wave velocity and Shear Modulus, Proc. 2nd ESOPT, 1982.

42) Uwabe, T., H. Tsuchida and E. Kurata: Coupled hydrodynamic response analysis based on strong motion earthquake records of fill type breakwater in deep sea, Report of the Port and Harbour Research Institute, Vol.22, No.2, pp.289-326, 1983 (in Japanese with English abstract)

43) Ichii, K., S. Iai and T. Morita: Effective stress analysis of the mechanism of deformation in caisson type quay walls, Proceedings of the symposium on the Great Hanshin Awaji Earthquake Disaster, Japan Society of Civil Engineers, pp.397-404, 1996 (in Japanese with English abstract).

44) Kokusho, T., A. Sakurai and Y. Esashi : Development of dynamic triaxial tests from small to large strain and their application to sands, Proceedings of the 14th Japan National Conference on Soil Mechanics and Foundation Engineering, Sapporo, pp.513-516, 1979 (in Japanese).

45) Usui, H., M. Kazama and T. Inatomi: The influence of shear modulus of soils depended on confined pressure on the results of 1D equivalent linear seismic response analysis, Proceedings of the Symposium on Response of Soils and Geotechnical Structures during Earthquakes, the Japan Society of Soil Mechanics and Foundation Engineering, Tokyo, pp.219-224, 1989 (in Japanese).

46) National Astronomical Observatory of Japan (ed): Chronological Scientific Tables, 2017 (in Japanese).

47) Usami, T.: Materials for Comprehensive List of Destructive Earthquakes in Japan, [416]-2001, Latest Edition, University of Tokyo Press, 2003 (in Japanese).

48) Sato, R. (ed): Handbook of Earthquake Fault Parameters in Japan, Kajima Institute Publishing, 1989 (in Japanese).

49) The Research Group for Active Faults of Japan, Active Faults in Japan: Sheet Maps and Inventories, Revised Edition, University of Tokyo Press, 1991 (in Japanese).

50) Nakata, T. and T. Imaizumi, Digital Active Fault Map of Japan, University of Tokyo Press, 2000 (in Japanese).

51) Takemura, M.: Scaling law for Japanese intraplate earthquakes in special relations to the surface faults and the damages, Zisin, 2nd series, Vol.51, pp.211-228, 1998 (in Japanese with English abstract).

52) Utsu, T.: Catalog of large earthquakes in the region of Japan from 1885 through 1980, Bulletin of the Earthquake Research Institute, Vol.57, pp.401-463, 1982.

53) Kanamori, H. (ed): Physics of Earthquakes, Iwanami Shoten Publishers, 1991 (in Japanese).

54) Kataoka, S., T. Kusakabe, J. Murakoshi and K. Tamura: Study on a procedure for formulating level 2 earthquake motion based on scenario earthquakes, Research Report of National Institute for Land and Infrastructure Management, No.15, 2003 (in Japanese with English abstract).

55) Esherby, J.D.: The determination of the elastic field of an ellipsoidal inclusion and related problems, Proc. Roy. Soc. Lond., Ser. A 241, pp.376-396, 1957.

56) Nozu, A.: A super asperity model for the 2011 off the Pacific coast of Tohoku earthquake, Journal of Japan Association for Earthquake Engineering, Vol.12, No.2, pp.21-40, 2012 (English translation is available in Vol.14, No.6).

57) Nozu, A. and A. Wakai: A source model for the 2011 off the Pacific coast of Tohoku, Japan, earthquake to explain strong ground motions, Report of the Port and Airport Research Institute, Vol.51, No.1, pp.23-53, 2012 (in Japanese with English abstract).

58) Irikura, K.: Recipe for predicting strong ground motion from future large earthquake, Annuals, Disaster Prevention Research Institute, Kyoto University, No.47A, pp.25-46, 2004 (in Japanese with English abstract).

59) Somerville, P.G., K. Irikura, R. Graves, S. Sawada, D. Wald, N. Abrahamson, Y. Iwasaki, T. Kagawa, N. Smith and A. Kowada: Characterizing crustal earthquake slip models for the prediction of strong ground motion, Seismological Research Letters, Vol.70, pp.59-80, 1999.

60) Irikura, K. and H. Miyake: Prediction of strong ground motions for scenario earthquakes, Journal of Geography, Vol.110, No.6, pp.849-875, 2001 (in Japanese with English abstract).

61) Irikura, K. and H. Miyake: Source modelling for prediction of strong ground motions, Chikyu Monthly, No.37, pp.62-77, 2002 (in Japanese).

62) Nozu, A.: An example of strong motion evaluation for a scenario earthquake with M_w9.0 along the Nankai trough with the SPGA model, Journal of JSCE, A1, Vol.69, No.4, pp.I_872-I_888, 2013 (in Japanese with English abstract).

63) Nozu, A. and A. Wakai: Application of SPGA model to strong motion estimation for a scenario earthquake with M_w9.0 along the Nankai trough, Technical Note of the Port and Airport Research Institute, No.1271, 2013 (in Japanese with English abstract).

64) Investigation Team for Modelling of Huge Subduction Earthquake along the Nankai Trough, Cabinet Office, Japan: On the seismic intensity distribution and tsunami heights due to an anticipated huge subduction earthquake along the Nankai trough, 1st report, http://www.bousai.go.jp/jishin/nankai/model/pdf/1st_report.pdf, 2012 (in Japanese).

65) Nozu, A., A. Wakai and Y. Nagasaka: Strong motion simulation for the 2011 off the Pacific coast of Tohoku earthquake – With considerations of soil nonlinearity –, Technical Note of the Port and Airport Research Institute, No.1284, 2014 (in Japanese with English abstract).

66) Takemura, M.: Magnitude-seismic moment relations for the shallow earthquakes in and around Japan, Zisin, 2nd series, Vol.43, pp.257-265, 1990 (in Japanese with English abstract).

67) Irikura, K.: Prediction of strong acceleration motions using empirical Green's functions, Proc. 7th Japan Earthq. Eng. Symp., pp.151-156, 1986.

68) Takemura, M. and T. Ikeura: A semi-empirical method using a hybrid stochastic and deterministic fault models: Simulation of strong ground motions during large earthquakes, J. Phys. Earth, Vol.36, pp.89-106, 1988.

69) Dan, K., T. Watanabe and T. Tanaka: A semi-empirical method to synthesize earthquake ground motions based on approximate far-field shear-wave displacement, Journal of Structural and Construction Engineering, AIJ, No.396, pp.27-36, 1989.

70) Kamae, K., K. Irikura and Y. Fukuchi: Prediction of strong ground motion based on scaling law of earthquake by stochastic synthesis method, Journal of Structural and Construction Engineering, AIJ, No.430, pp.1-9, 1991 (in Japanese with English abstract).

71) Kamae, K., K. Irikura and A. Pitarka: A technique for simulating strong ground motion using hybrid Green's function, Bulletin of the Seismological Society of America, Vol.88, pp.357-367, 1998.

72) Matsushima, S. and H. Kawase: Multiple asperity source model of the Hyogo-ken Nanbu earthquake of 1995 and strong motion simulation in Kobe, Journal of Structural and Construction Engineering, AIJ, No.534, pp.33-40, 2000 (in Japanese with English abstract).

73) Science and Technology Agency, Japan: Proceedings of the 1st Symposium on Investigation Results of Subsurface Structure of Sedimentary Basins, 2000 (in Japanese).

74) Kowada, A., M. Tai, Y. Iwasaki and K. Irikura: Evaluation of horizontal and vertical strong ground motions using empirical site-specific amplification and phase characteristics, Journal of Structural and Construction Engineering, AIJ, No.514, pp.97-104, 1998 (in Japanese with English abstract).

75) Boore, D.M.: Stochastic simulation of high-frequency ground motions based on seismological models of the radiated spectra, Bulletin of the Seismological Society of America, Vol.73, pp.1865-1894, 1983.

76) Brune, J.N.: Tectonic stress and the spectra of seismic shear waves from earthquake, J. Geophys. Res., Vol.75, pp.4997-5009, 1970.

77) Brune, J.N.: Correction, J. Geophys. Res., Vol.76, p.5002, 1971.

78) Satoh, T. and Y. Tatsumi: Source, path and site effects for crustal and subduction earthquakes inferred from strong motion records in Japan, Journal of Structural and Construction Engineering, AIJ, No.556, pp.15-24, 2002 (in Japanese with English abstract).

79) Tsurugi, M., S. Sawada, M. Miyajima and M. Kitaura: Re-estimation of site amplification effects in Kansai region, Journal of Structural Engineering, Vol.48A, pp.577-586, 2002 (in Japanese with English abstract).

80) Kato, K: Evaluation of source, path, and site amplification factors from the K-NET strong motion records of the 1997 Kagoshima-ken-hokuseibu earthquakes, Journal of Structural and Construction Engineering, AIJ, No.543, pp.61-68, 2001 (in Japanese with English abstract).

81) Iwata, T. and K. Irikura: Separation of source, propagation and site effects from observed S-waves, Zisin, 2nd series, Vol.39, pp.579-593, 1986 (in Japanese with English abstract).

82) Irikura, K., T. Kagawa and H. Sekiguchi: Revision of the empirical Green's function method by Irikura (1986), Programme and Abstracts, The Seismological Society of Japan, B25, 1997 (in Japanese).

83) Aki, K. and P.B. Richards: Quantitative Seismology, Second Edition, University Science Books, 2002.

84) Miyake, H., T. Iwata and K. Irikura: Source characterization for broadband ground-motion simulation: kinematic heterogeneous source model and strong motion generation area, Bulletin of the Seismological Society of America, Vol.93, pp.2531-2545, 2003.

85) The Research Group for Theoretical Ground Motions: Earthquake Ground Motions – Synthesis and Analysis, Kajima Institute Publishing, 1994 (in Japanese).

86) Nozu, A., T. Annaka, Y. Sato and T. Sugano: Characteristics of ground motions observed at Haneda Airport (First report) Characteristics of surface waves, Technical Note of the Port and Airport Research Institute, No.1022, 2002 (in Japanese with English abstract).

87) Nozu, A., H. Takahashi and T. Endoh: Apparent velocity of seismic waves traveling along shield tunnel evaluated based on earthquake observation, Journal of JSCE, A1, Vol.66, No.1, pp.61-72, 2010 (in Japanese with English abstract).

2 Crustal Deformations

When a large earthquake occurs, the fault movement causes an elastic crustal deformation and may result in a permanent displacement of the ground in a large surrounding area. This is called a crustal deformation.

The displacement can include horizontal and vertical components and the latter can be in the upward or downward directions depending on the direction of the fault movement and the relative location of the construction site with respect to the fault. In recent years, a subsidence of 1.2 m occurred in the Oshika Peninsula during the 2011 Tohoku earthquake[1)]. During the 1707 Hoei earthquake, downtown Kochi suffered a subsidence of 2 m at maximum, while in Murotsu, an uplift of 1.8 m occurred and the port became unable to accommodate large ships[2)].

Regarding crustal deformations due to an earthquake, the following issues should be considered upon necessity.

① If an uplift associated with a crustal deformation occurs at a port, a shortage can occur in the water depth of a high seismic resistant quay wall for emergency transport. Therefore, when a high seismic resistant quay wall for emergency transport is planned at a port where the occurrence of a huge subduction earthquake is anticipated, it is preferable to plan the quay wall so that it can maintain a sufficient water depth after the occurrence of the uplift by carefully examining the possibility and amount of the uplift. The same applies to related waterways and basins.

② If a subsidence associated with a crustal deformation occurs at a port, a shortage can occur in the height of a revetment or a coastal dike that constitutes part of countermeasures against a tsunami. In addition, an increase can occur in the tsunami force. Therefore, when those facilities are constructed at a port where the occurrence of a huge subduction earthquake is anticipated, it is preferable to plan those facilities so that they can maintain a sufficient height after the occurrence of the subsidence and to consider possible increase in the tsunami force due to the subsidence upon necessity, based on sufficient study on the possibility and amount of the subsidence.

Although the direction and amount of the permanent displacement associated with a crustal deformation can be calculated numerically considering the location and size of the anticipated earthquake, they can also be determined by referring to the amount of permanent displacements during large historical earthquakes in the region. For example, the amount of the uplift and subsidence during past great earthquakes along the Nankai trough is reported by Usami[2)].

However, historical data is not always available at a given port. In addition, huge subduction earthquakes greater than regional historical earthquakes are considered in tsunami simulations more often than ever. Therefore, it is necessary to numerically calculate the permanent displacement associated with the crustal deformation if historical data is not available at the port under consideration or a huge subduction earthquake greater than regional historical earthquakes is considered. For this calculation, the analytical solution for the elastic deformation of a half space[3)] is often used. A computer program for this calculation is provided by the National Research Institute for Earth Science and Disaster Resilience, Japan[4)]. It is important to make sure that the hypothesized slip distribution for the calculation of the permanent displacement is consistent with that assumed for the tsunami simulations. For anticipated great earthquakes along the Nankai trough, the direction and amount of the permanent displacements associated with a crustal deformation are also hypothesized by the Cabinet Office and are available for the design.

Permanent displacements associated with postseismic crustal deformations, which gradually occur for years after the occurrence of a great earthquake, can be in an opposite direction to those associated with coseismic crustal deformations, which occur at the moment of the earthquake. For example, in the Oshika Peninsula, in the five years following the 2011 Tohoku earthquake, an uplift equivalent to approximately 40% of the coseismic subsidence occurred[5)]. This tendency was due to the fact that, while the coseismic slip occurred relatively offshore, the postseismic slip occurred near the coast. It should be noted that the tendency can be significantly region dependent; it is not reasonable to assume the same tendency for different regions.

[References]

1) Geospatial Information Authority of Japan: Crustal deformations observed at continuously operating GNSS reference stations, Information regarding the 2011 Tohoku earthquake, https://www.gsi.go.jp/chibankansi/chikakukansi40005.html, 2011(in Japanese).

2) Usami, T.: Materials for Comprehensive List of Destructive Earthquakes in Japan, [416]-2001, Latest Edition, University of Tokyo Press, 2003 (in Japanese).

3) Okada, Y.: Surface deformation due to shear and tensile faults in a half-space, Bull. Seism. Soc. Am., Vol.75, pp.1135-1154, 1985.

4) National Research Institute for Earth Science and Disaster Resilience, Japan: Program to calculate deformation due to a fault model DC3D0/DC3D, http://www.bosai.go.jp/study/application/dc3d/DC3Dhtml_E.html.

5) Geospatial Information Authority of Japan: Observation results by the GEONET, Five years after the 2011 Tohoku earthquake, http://www.gsi.go.jp/kanshi/h23touhoku_5years.html, 2016 (in Japanese).

3 Seismic Actions

3.1 Modeling of Soil-structure System and Seismic Actions

In the following, various analysis methods for the performance verification of port structures against earthquakes and associated seismic actions will be explained.

First, the difference of “earthquake ground motions” and “seismic actions” will be explained based on the descriptions in ISO23469[1)]. Earthquake ground motions can exist where there is no structure, however, seismic actions can only exist when there is a structure. For example, an inertia force acting on a deck of a pile-supported wharf, which is an example of a seismic action, can only exist when there is a deck. Similarly, a seismic earth pressure acting on a wall, which is also an example of a seismic action, can only exist when there is a wall.

According to ISO23469[1)], “seismic actions” can be differently defined for the same structure depending on the analysis method. For example, if a “caisson” is considered and its stability against sliding is examined as in **Fig.3.1.1 (a)**, the external forces acting on the caisson such as the inertia force, the seismic earth pressure and the hydrodynamic pressure can be defined as the seismic actions. However, if the response of a soil-structure system composed of a caisson, backfill soils, foundation soils and sea water is analyzed as in **Fig. 3.1.1 (b)**, the seismic earth pressure and the hydrodynamic pressure are not seismic actions; they are obtained as a result of the response analysis. In this case, the seismic actions are the earthquake ground motions specified at the bottom of the analysis domain. In both **Figs.3.1.1 (a)** and **(b)**, the analysis domain is shown by the shaded area and the “seismic actions” are defined at its boundary.

If part of a soil-structure system is considered as in **Fig. 3.1.1 (a)**, the analysis is called a simplified analysis. If the response of a whole system is considered as in **Fig.3.1.1 (b)**, the analysis is called a detailed analysis (**Table 3.1.1**). Each of these analyses involves static and dynamic analyses. As a result, analysis methods for the performance verification against earthquakes can be classified into 2×2=4 categories (**Table 3.1.1**). Among various analysis methods below, the seismic coefficient method, the modified seismic coefficient method and the seismic displacement method can be categorized as static simplified analyses. The earthquake response analyses of a soil-structure system such as the effective stress analyses can be categorized as dynamic detailed analyses.

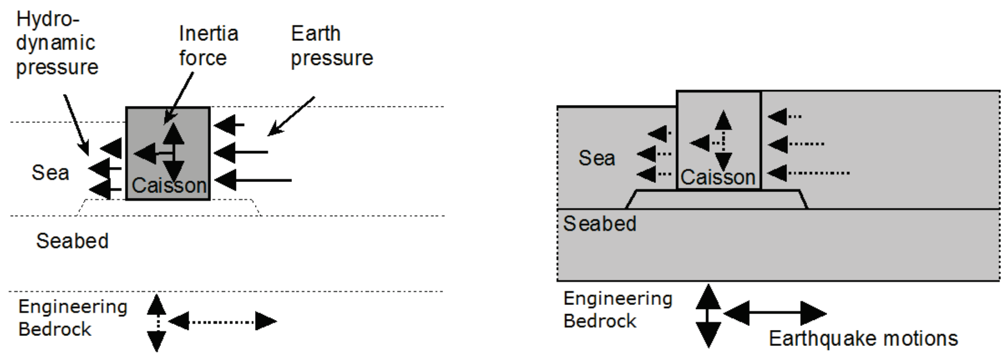

(a) Simplified analysis (*e.g.*, seismic coefficient method) (b) Detailed analysis (*e.g.*, effective stress analysis)

Fig. 3.1.1 Seismic actions in a simplified and detailed analysis

Table 3.1.1 Various analysis methods for the performance verification of port structures against earthquakes

	Simplified analysis	Detailed analysis
Static analysis	Static simplified analysis - Seismic coefficient method (**3.2**) - Modified seismic coefficient method (**3.3**) - Seismic displacement method (**3.4**)	Static detailed analysis - Static analysis of a soil-structure system
Dynamic analysis	Dynamic simplified analysis - Newmark method	Dynamic detailed analysis - Earthquake response analysis of a soil-structure system (**3.5**) (*e.g.*, effective stress analysis)

3.2 Seismic Actions for Seismic Coefficient Method[2)]

Assume a rigid body on a rigid ground as shown in **Fig. 3.2.1**. Let m and W (=mg) denote the mass and the weight of the rigid body, respectively, where g stands for the acceleration of gravity. When the ground moves with a rightward acceleration of α, the body will be subject to a leftward inertia force of $m\alpha$. In order for the rigid body not to slide, a friction force of $m\alpha$ should act at the bottom of the rigid body. If the static friction coefficient at the bottom is not sufficiently large, a sliding occurs and often results in a residual displacement, although the occurrence of the residual displacement could depend on the change of the acceleration afterwards. The occurrence of the sliding can be examined by applying a static force of $m\alpha$ on the rigid body. This is the basic idea of the seismic coefficient method.

The inertia force F applied in the seismic coefficient method can be written as follows:

$$F = (\alpha/g)W \tag{3.2.1}$$

By replacing α/g with k_h, one obtains the following expression:

$$F = k_h W \tag{3.2.2}$$

The equation implies that, if the weight is multiplied by the coefficient k_h, it yields the inertia force due to the earthquake ground motion. The coefficient k_h is called the "seismic coefficient". The seismic coefficient determined for the performance verification of a structure is called the "seismic coefficient for performance verification". The "seismic coefficient" is completely different from the "seismic intensity" announced by the Japan Meteorological Agency, although they are both pronounced in the same way as "shindo" in the Japanese language.

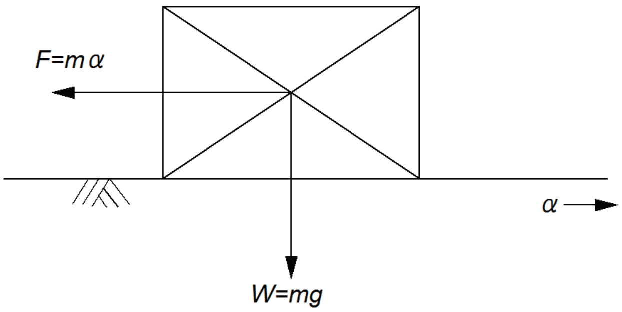

Fig. 3.2.1 Concept of seismic coefficient method

The seismic coefficient method was proposed in 1916 by Sano[3)]. According to the categorization in **Part II, Chapter 6, 3.1 Modeling of Soil-structure System and Seismic Actions**, the seismic coefficient method can be categorized as a static simplified analysis. The method has widely been used not only for port structures but also for other structures because, in the method, the problem of the seismic stability of a structure can be easily analyzed by replacing it with a problem of the equilibrium of static forces. For port structures, the method is used for the performance verification of gravity quay walls, sheet-pile quay walls, cell-type quay walls, etc. for level-1 ground motions. When the method is applied to a gravity quay wall, in addition to the inertia force on the wall, the seismic earth pressure and the hydrodynamic pressure should be considered as shown in **Fig.3.1.1 (a)**.

In the performance verification for a level-1 ground motion, if the ratio of the peak ground acceleration with respect to the acceleration of gravity is selected as the seismic coefficient, the value of the seismic coefficient will become much larger than the values usually used in the design. In fact, it is not necessary to directly adopt the ratio as the seismic coefficient. For example, if α=215 Gal, **equation (3.2.1)** yields k=0.22. However, it is empirically known[2)4)] that a ground motion exceeding 215 Gal does not necessarily cause a residual displacement to a quay wall designed with a seismic coefficient of 0.22. This is presumably due to the fact that, even if the quay wall is subject to a ground motion exceeding 215 Gal, as long as the duration of the action is short, it will not cause any visible residual displacement of the quay wall. The conversion method from the acceleration time history of a level-1 ground motion to the seismic coefficient for performance verification depends on the type of the structure. Details can be found in **Reference (Part III), Chapter 1, 1 Details of Seismic Coefficient for Performance Verification.**

The seismic coefficient method generally assumes that the backfill and foundation soils of a wall do not liquefy. The seismic earth pressures and the material properties of the foundation soils are given based on this assumption. Therefore, if the performance verification for a level-1 ground motion is conducted with the seismic coefficient method, the possibility of liquefaction of the backfill and foundation soils should be assessed and, if the occurrence of liquefaction is anticipated, countermeasures against liquefaction should be taken (see **Part II, Chapter 7, Liquefaction**).

Because of the basic concept of the seismic coefficient method, it can assess the occurrence of the deformation of a structure following a few prescribed modes such as sliding, overturning and instability of the foundation soil based on the equilibrium of static forces, however, the method cannot estimate the amount of residual deformation once it occurs. Because of this limitation of the seismic coefficient method, it is not realistic to apply the seismic coefficient method to a level-2 ground motion. In general, for a very strong ground motion such as a level-2 ground motion, under the premise that certain amount of damage is inevitable, the performance of an infrastructure should be assessed considering the damage process[5)6)]. The same applies to a port facility such as a mooring facility; for a level-2 ground motion, under the premise that certain amount of residual deformation occurs, a facility should be designed so that the amount of deformation does not exceed a prescribed allowable value. To meet such requirements, instead of simplified analyses based on the seismic coefficient method, earthquake response analyses of a soil-structure system should be conducted as explained later.

3.3 Seismic Actions for Modified Seismic Coefficient Method[2)]

The seismic coefficient method assumes that the ground and the structure move together as shown in **Fig. 3.2.1**, however, in the case of a flexible structure, the acceleration of the structure α' does not coincide with that of the ground α as shown in **Fig. 3.3.1**. In this case, once the dynamic characteristics of the structure such as the natural period and the time history of the ground acceleration are given, the time history of the response acceleration can be calculated and, by applying a static force equivalent to the peak response acceleration multiplied by the mass *m* to the structure, the seismic design can be conducted by replacing actual dynamic phenomena with the equilibrium of static forces. The seismic coefficient method thus expanded to a flexible structure is called the "modified seismic coefficient method". Once the time history of a ground acceleration is given, the time history of the response acceleration can be calculated for structures with various natural periods and the peak response acceleration can be plotted as a function of the natural period. This plot is called a "spectral acceleration".

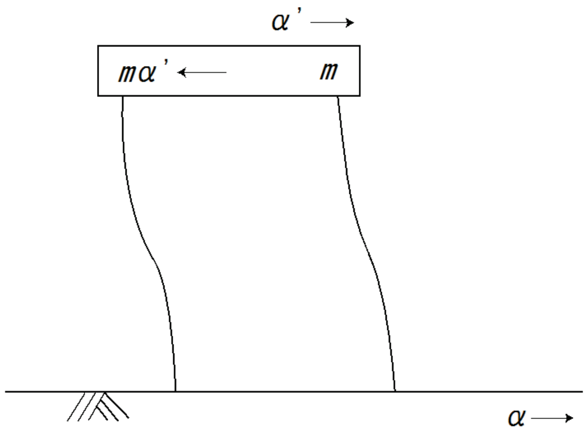

Fig. 3.3.1 Concept of modified seismic coefficient method

According to the categorization in **Part II, Chapter 6, 3.1 Modeling of soil-structure system and seismic actions**, the modified seismic coefficient method can be categorized as a static simplified analysis. In the modified seismic coefficient method, a linear restoring force is often assumed to calculate the response of the structure. However, when the structure is subject to a very strong ground motion, the restoring force of the structure shows a nonlinear behavior due to the yielding of its members. In that case, the response acceleration calculated by assuming a linear response becomes meaningless. Thus, the modified seismic coefficient method is not suitable for a very strong ground motion such as a level-2 ground motion.

3.4 Seismic actions for seismic displacement method[2)]

In designing a long structure with less apparent density and rigidity such as a buried pipeline or a submerged tunnel, the acceleration induced in the structure is less important in the design. Because of its less density and rigidity, its existence has little effects on the displacement of the surrounding ground; the displacement of the structure tends to be governed by the displacement of the ground. If the displacement of the ground is not uniform, strain is induced in the structure, which becomes an important issue in the design.

In the seismic displacement method, first, the displacement of the ground is calculated without considering the existence of the structure. Next, the displacement and stress of the structure are calculated by assuming that the displacement of the structure follows that of the ground. Thus, in contrast to the seismic coefficient method where a static force is applied to a structure as a seismic action, in the seismic displacement method, the displacement of the ground is applied to a structure as a seismic action. If the rigidity of the structure is slightly large, the assumption that the displacement of the structure follows that of the ground may lead to an error. In that case, the displacement of the ground is applied to a structure via springs. According to the categorization in **Part II, Chapter 6, 3.1 Modeling of Soil-structure System and Seismic Actions**, the seismic displacement method can be categorized as a static simplified analysis.

3.5 Seismic Actions for Earthquake Response Analysis of Soil-structure System

In each of the above mentioned methods, the actual phenomena are more or less simplified. However, earthquake response analyses are sometimes conducted aimed at examining a more realistic response of a soil-structure system. This type of analysis can be categorized as a dynamic detailed analysis according to the categorization in **Part II, Chapter 6, 3.1 Modeling of Soil-structure System and Seismic Actions**. Earthquake response analyses of a soil-structure system are often based on finite element analyses, especially on effective stress analyses as shown in **Fig. 3.5.1**. In this case, the seismic actions are the earthquake ground motions specified at the bottom of the analysis domain.

In general, the ground motion at the bottom of the analysis domain is the sum of the upcoming (E) and downgoing (F) waves. There are two methods to specify the ground motion at the bottom of the analysis domain: One is to specify the ground motion to be observed at the bottom of the analysis domain (E+F). The other is to specify the incident wave impinging at the bottom of the analysis domain multiplied by 2 (2E). In the event of reproducing actual damage in a past earthquake or reproducing the results of shake table tests, the observed ground motion at the bottom of the analysis domain including the effects of the upcoming and downgoing waves (E+F) may be available. In that case the E+F wave can be specified. However, in an earthquake response analysis of a soil-structure system for the performance verification of a structure, a 2E wave should be specified. If the analysis domain is just above the engineering bedrock, the ground motion obtained in **Part II, Chapter 6, 1 Earthquake Ground Motions** can be directly used. However, if the analysis domain is not in contact with the engineering bedrock, the ground motion defined at the engineering bedrock should be converted to a 2E wave just below the analysis domain by conducting an earthquake response analysis of the ground and used.

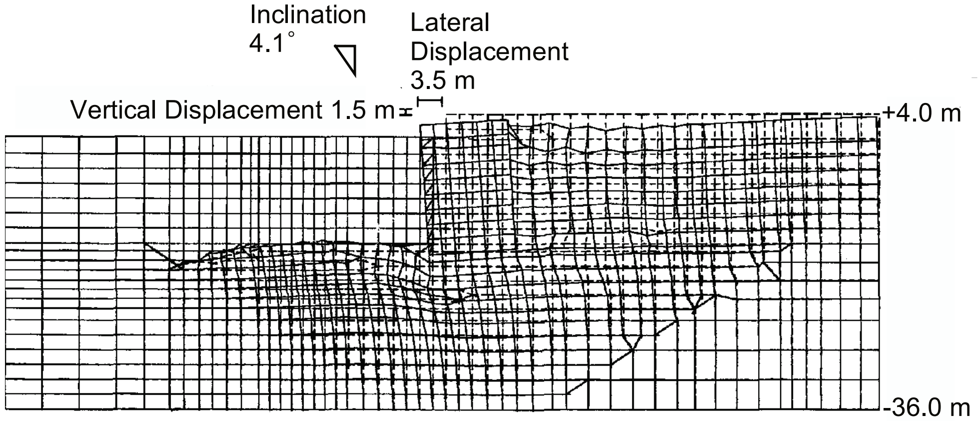

Fig. 3.5.1 Deformation of a gravity quay wall calculated by an effective stress analysis

[References]

1) International Organization for Standardization: ISO23469, Bases for design of structures - Seismic actions for designing geotechnical works, 2005.
2) Tsuchida, H. and S. Iai: Earthquake Engineering for Practitioners, Sankaido, 1991 (in Japanese).
3) Sano, R.: Earthquake resisting structure of houses, Reports of the Imperial Earthquake Investigation Committee, Vol.83, 1916 (in Japanese).
4) Noda, S., T. Uwabe and T. Chiba: Relation between seismic coefficient and ground acceleration for gravity quaywall, Report of the Port and Harbour Research Institute, Vol.14, No.4, pp.67-111, 1975 (in Japanese with English abstract).
5) Japan Society of Civil Engineers: Proposal on seismic design standards for infrastructures, 1996 (in Japanese).
6) Japan Society of Civil Engineers: Proposal and commentary on seismic design standards for infrastructures: the third proposal, 2000 (in Japanese).